UNIVERSITY OF CINCINNATI

Date: January, 21, 2004

I, Mina Tsunakawa ,

hereby submit this work as part of the requirements for the degree of:

Master of Science

in:

Department of Chemical Engineering

It is entitled:

Novel Three-Coordinate Mo(III) Complexes for Nitrogen Removal from Flue Gas under Ambient Conditions

This work and its defense approved by:

Chair:

Dr. Vadim Guliants

Dr. Rakesh Govind

Dr. Neville Pinto

Novel Three-Coordinate Mo(III) Complexes for Nitrogen Removal from Flue Gas under Ambient Conditions

A thesis submitted to the

Division of Research and Advanced Studies

of the University of Cincinnati

in partial fulfillment of requirements for the degree of

Master of Science

in the Department of Chemical Engineering

of the College of Engineering

2004

by:

Mina Tsunakawa

B. S., Gunma University, 1992

M. S., Gunma University, 1994

Committee:

Dr. Vadim Guliants

Dr. Rakesh Govind

Dr. Neville Pinto

Abstract

Reducing CO_2 emissions from flue gas is becoming significantly important due to its impact on global climate change. CO_2 from large stationary sources such as coal-fired power plants is mixed with nitrogen, water vapor, oxygen, and other gaseous (e.g. NO_x and SO_x) and particulate impurities. In most cases, N_2 comprises about 70% of flue gas and multiple discrete separation steps are required to remove CO_2 and various gas impurities from N_2. As a result, the current flue gas treatment technology is very expensive. Therefore, there is a critical need for novel economical and energy-conserving technologies for one-step separation of CO_2 and other gas impurities from N_2 in flue gas.

We proposed novel three-coordinate Mo(III) complexes $Mo(N[R]Ar)_3$ for selective removal of N_2 from flue gas. These novel three-coordinate Mo(III) complexes have a unique ability to selectively adsorb N_2. The Mo(III) complex was synthesized according to modified synthesis procedures. ^{1}H-NMR, GC-MS and TOFMS were used for the identification of various intermediate compounds and the final complexes. The target Mo(III) complex was successfully synthesized. However, the Mo(III) complex exhibited limited stability upon exposure to the air or moisture. Therefore, study of adsorption and desorption of N_2, CO_2, and other gas impurities was not feasible. In conclusion, we discuss several approaches to stabilize these N_2-binding Mo complexes for practical application on CO_2 separation from flue gas.

Acknowledgement

This study was sponsored by Ohio Coal Development Office (OCDO). Their financial support is deeply acknowledged. I would like to show my deep gratitude to my adviser, Dr. Vadim Gulians for his guidance, suggestions and help throughout this study. Sincere appreciation and gratitude go to Dr. Rakesh Govind and Dr. Neville Pinto for their participation on my committee. I am very grateful to Dr. Allan Pinhas for useful advice in organic synthesis, and for allowing me to use one of his laboratories for this study. My thanks also go to Dr. Junichi Ida for his enormous help in setting up the laboratory. I would also like to thank Dr. Matthew Hancock for teaching me the experimental techniques in organic synthesis. I thank Dr. Elwood Brooks for adjusting ^{1}H-NMR spectrometer for paramagnetic chemical shifts measurement even though the machine was not made for the purpose. I also wish to express my gratitude to these people in my laboratory who helped me and cheered me up:

Dr. Moises Carreon, Mr. Sangil Kim, Mr. Sanjay Sarang, Mr. Parveen Kumar, Ms. Li Yuan, and Mr.Rishabh Bhandari.

Lastly, I would like to thank my husband, Satoshi Tsunakawa, for his helpful discussions and constant encouragement behind scenes.

Table of Contents

List of Figures

List of Tables

Chapter 1

Introduction

1.1 Problem Statement

Concerns over the increased concentration of CO_2 in the atmosphere and its effect on global climate change have increased the awareness and investigation for reducing CO_2 emissions. A number of mitigation technologies, including CO_2 sequestration (geological, ocean and terrestrial) and novel CO_2 utilization, are currently under investigation [1-4]. Most of these processes require CO_2 in a concentrated form. However, the CO_2 from large sources such as coal-fired power plants is mixed with nitrogen, water vapor, oxygen, and other elemental (e.g. SO_x and NO_x) and particulate impurities and present at ~15% concentration. In many CO_2 sequestration schemes, a number of discrete separation steps are employed to remove various gas impurities and CO_2 from N_2, which is a majority component in flue gas. For example, these steps include an SCR unit to remove NO_x, a wet scrubber to remove SO_x, and would include an additional unit, most likely located either before or after a wet scrubber, to concentrate CO_2 from a wet N_2 stream. As a result, these schemes are quite expensive with high associated capital and process costs. Therefore, there is a critical need for novel economical and energy-conserving technologies for one-step separation of CO_2 and other gas impurities from N_2 in flue gas.

1.2 Current Technologies

1.2.1 Liquid Amine Sorbents

A chemical absorption method with monoethanol amine (MEA) as the sorbent is used for current commercial operations for capturing carbon dioxide from flue gas [5, 6]. The reaction is taking place in between 2 moles of MEA and 1 mole of CO_2 [Equation

(1)] , while in the presence of water, one mole of amine can reacts with 1 mole of carbon dioxide [Equation (2)] [6].

$$2RNH_2 + CO_2 \rightarrow RNH_3^+ + RNHCO_2^- \quad (1)$$

$$RNH_2 + CO_2 + H_2O \rightarrow RNH_3^+ + HCO_3^- \quad (2)$$

Liquid amines are widely used for carbon dioxide removal but it is expensive and energy intensive process because of following reasons:

(i) MEA needs high heat for absorption with CO_2.

(ii) The strong binding between CO_2 and MEA requires high regeneration energy.

(iii) MEA is degraded by miner components in the flue gas such as SO_2 and O_2, etc.

(iv) MEA is corrosive and only diluted solution can be used.

(v) Relatively high volatility of MEA causes vaporization loss.

To develop alternative technologies, various carbon dioxide capture methods, that include, steric hindrance amines [7], solid sorbents, membrane separation, and cryogenic separation are under testing.

1.2.2 Solid Amine and Metal Oxide Sorbents

Hamilton Sunstrand Space Systems International had developed a regenerable sorbent, known as HSC$^+$ [8]. The material consists of a polyethyleneimine, bonded to a high-surface area solid polymethyl methacrylate polymeric support. This sorbent had used in space life support, and it is expected to be used for CO_2 removal from flue gas. There has been also widespread interest in developing amine surface-bonded material such as silica gel and ordered mesoporous silica [9, 10]. These solid supports have large surface areas and high concentrations of silanol groups on their surfaces to graft

functional amine groups, so that high CO_2 adsorption capacities may be achievable. The key advantages of solid amine sorbents as opposed to liquid amines are ease of handling and their regenerability under mild conditions.

Metal oxide such as calcium oxide can be also used for separation of carbon dioxide from flue gas. The chemical reaction of CO_2 with solid metal oxide (represented by MO) forms metal carbonate [Equation (3)] [11, 12].

$$MO + CO_2 \rightarrow MCO_3 \qquad (3)$$

It can be thermally regenerated to metal oxide and carbon dioxide by hearting the metal carbonate, MCO_3 [Equation (4)].

$$MCO_3 \rightarrow MO + CO_2 \qquad (4)$$

Carbon dioxide separation using metal oxide provides the following advantages:

(i) Carbon dioxide separation can be conducted under flue gas condition, i.e., high temperature and atmospheric pressure.

(ii) The sorption capacity is higher than other technologies. For example, MEA captures 60 g of CO_2/kg, while CaO captures 400g of CO_2/kg.

(iii) Upon regeneration, pure CO_2 can be yielded.

1.2.3 Zeolite Sorbents

Generally, gas separation using zeolite is based on the difference in molecular size, and/ or interaction with intra zeolitic cations [19-22]. In case of CO_2/N_2 separation, the difference in size is very small, i.e., ~10%, so that the separation relies on the strength of interactions with intra zeolitic cations. N_2 molecules, which possess no permanent dipole moment and a very small quadrupole moment, interact very weakly with the

charged active sites as compared to CO_2, which possess a 3-fold greater quadrupole moment. However, this method suffers from extreme sensitivity to the presence of moisture.

1.2.4 Membrane Separation

Thin nonporous polymeric membranes are the only commercially successful membranes for gas separation [13, 14]. However, CO_2/N_2 selectivity is not high because the separation is simply based on the difference in permeation rates through the thin selective layer. To increase the selectivity of membrane, immobilize liquid membranes have been proposed.

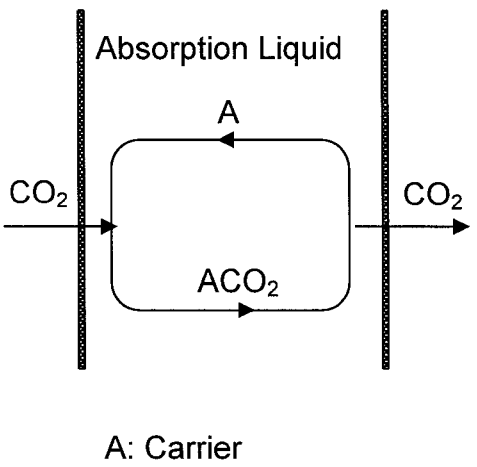

Figure 1. Liquid membrane separation of CO_2.

In liquid membranes, a carrier compound dissolved into a fluid, which is trapped physically in the pores of a porous polymer [15-17]. The carrier acts as a shuttle to selectively transport carbon oxide across the membrane. The principle is shown in Figure

1. Although this type of membrane can achieve high selectivity, the function can not last more than one month due to the evaporation of the fluid and the degradation of the carrier.

1.2.5 Cryogenic Separation

All gas species have a particular boiling temperature. Separation of gas mixtures using the difference in boiling points of various gas species is called cryogenic separation [18]. A gas being separated is cooled until it becomes a boiling liquid. In the case of carbon dioxide, its boiling point is -56.8°C at 1 atmosphere. The conditions are achieved via compression and heat exchange. Although this method can provide effective gas separation, it is very energy intensive technology because carbon dioxide concentration in flue gas is as low as 15%.

Most technologies to separate CO_2 and other gas impurities from N_2 in flue gas rely on the differences in either the molecular size or the strength of interactions between these molecules and the separation medium (e.g. a chemical absorbent, polymeric or membrane surface, or zeolite adsorbent). Kinetic separations based on the molecule size differences are all CO_2-selective, because CO_2 is ~10% smaller than nitrogen. This separation is expected to be even less efficient for NO_2 and SO_2 molecules, which possess similar and slightly greater molecular diameters than CO_2. Separations that rely on the different strength of interactions with the separation medium are again CO_2-selective. The current commercial operations for separating CO_2 from flue gas use a chemical absorption method with monoethanolamine (MEA), which relies on strong acid-base interactions between MEA and CO_2. Another reaction-based process is based

on the interiaction between CO_2 and metal oxide. Separation methods using zeolites rely on electrostatic interactions between CO_2 and zeolitic nonframework cations. Cryogenic gas separation is based on neither molecular size nor interaction with medium, but the difference in boiling point between gases. However, it is also CO_2-selective since boiling point of CO_2 and N_2 are -78.5°C and -195.8°C at 1 atmosphere, respectively.

The review of current and emerging technologies for CO_2 capture from flue gas demonstrates the lack of N_2-selective separation methods, which will enable N_2 separation from CO_2 and other gas impurities. Such separation is highly desirable as it may eliminate the need for an SCR to remove NO_x and a wet scrubber for the SO_x removal with associated capital and process costs. Therefore, there is a critical need for novel N_2-selective separation methods, that will provide high N_2/CO_2 separation selectivity ($\alpha > 60$) and, at same time, cost-effective and energy-efficient CO_2 capture from flue gas.

1.3 Research Objective

We propose here three-coordinate Mo(III) complexes for N_2-selective separation from CO_2 and other gas impurities in flue gas [23-28]. In a practical separation, these complexes can be attached to the surface of mesoporous silica membranes, which are expected to have long life, low manufacturing and operating costs, high permeance, rugged construction and non-fouling surfaces. The strength of the N_2 interaction, the N_2/CO_2 (and N_2/other acid gas) selectivity and N_2 flux in membrane-supported three-coordinate Mo(III) complexes can be fine-tuned by a proper selection of the complex ligand and the membrane pore size to provide the facilitated transport membranes with

optimal performance in N_2 separation from flue gas. The review of the prior art suggests that it is possible to achieve high N_2 separation selectivity, α (N_2/CO_2) ~ 80, and N_2 permeance, P ~ 10^{-6} mol/m^2 · s · Pa using three-coordinate Mo(III) complex-modified mesoporous silica membranes [23,24]. The goals of this MS research is to synthesize three-coordinate Mo(III) complexes and characterize its N_2 separation ability from CO_2 and other gas impurities.

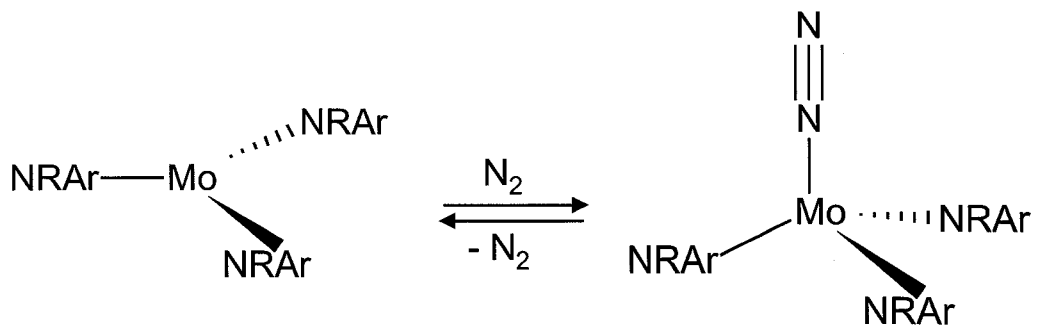

Figure 2. Three-coordinate Mo(III) complexes for selective N_2 adsorption [28].

1.4 Estimation of Specific Economic Advantages in Membrane Separation Methods Employing the Mo(III) complexes

Our preliminary estimates summarized in Table 1 indicate that it may be possible to achieve capture costs in the $10/ton of CO_2 range employing this novel membrane technology. The N_2/CO_2 selectivity and the N_2 permeance can be fine-tuned by a proper selection of the Mo(III) complex and the pore size to provide the membranes with optimal performance in N_2 separation from flue gas. These membranes can be operated at low temperatures (50-160°C) in the presence of water and other gas impurities and are expected to concentrate CO_2 from 15 to over 90%. The major potential advantage of this novel membrane technology is that the gas impurities, such as SO_x and NO_x, may also be

selectively removed from flue gas along with CO_2, thereby eliminating the need for an SCR and a wet scrubber with associated capital and process costs. Therefore, this novel separation technology has a potential to compete with the chemical absorption method, which utilizes liquid amines.

Power plant size[1]	1000-1300 MW
Annual CO_2 emissions	9.6-12.5 mln ton
CO_2 in flue gas	12-15%
p (flue gas)	1.0 atm
Δp	0.5 atm
N_2/CO_2 selectivity	80
N_2 permeance	2.5 μmol/m^2·s·Pa
Membrane+support	(160-208 kg) + (160-208 ton)
Membrane+support cost[2]	$200/kg
Hardware cost (piping, pressure/flow control)	$840K
Hardware cost	$34-44M
Fan power cost	$6.9-8.6/ton of CO_2
Total capture cost	$10.5-12.2/ton of CO_2

[1] From "Carbon Dioxide Emissions from the Generation of Electric Power in the United States", DOE Energy Information Administration, Form EIA-412, "Annual Report of Public Electric Utilities", 1998.

[2] conservative estimate of annual manufacturing cost.

Table 1. Cost estimates of CO_2 capture employing novel Mo(III) complex-modified membranes.

Chapter 2

Literature Review

2.1 Nitogenase and Other Dinitrogen Metal Complexes

Certain types of enzyme called nitrogenase can fix dinitrogen at ambient temperature and atmospheric pressure. Nitrogenases generally contain transition metals such as Fe, Mo, and V at their catalytically active site [29-32]. Thus, there is a wide interest in dinitrogen fixation by metal complexes since it can be considered a new pathway to produce ammonia. Since the discovery of the first dinitrogen complex $Ru(NH_3)_5(N_2)^+$ [33], a large number of dinitrogen complexes consisting of different transition metals or different ligands have been synthesized and studied. Generally the synthetic routes to dinitrogen complexes have been limited to these three categories.

2.1.1 Replacement of Ligand with Dinitrogen

The reaction of dinitrogen with a complex involves replacement of labile ligands by dinitrogen. Treatment of the dihydride $MoH_4(dppe)_2$ with dinitrogen at 1 atmospher gives $Mo(N_2)_2(dppe)_2$, (dppe = 1,2-bis(diphenylphosphino)ethane) by replacement of H_2 with N_2 [Equation (5)] [34, 35].

$$MoH_4(dppe)_2 + 2N_2 \rightarrow Mo(N_2)_2(dppe)_2 + 2H_2 \qquad (5)$$

Several dinitrogen complexes of chromium containing cyclic hydrocarbon ligands are generally prepared by replacement of a labile ligand such as cyclopentene with dinitrogen [Equation (6)] [36].

$$Cr(\eta^6\text{-}C_6H_6)(CO)_2(\eta^2\text{-}C_5H_8) + N_2 \rightarrow Cr(\eta^6\text{-}C_6H_6)(CO)_2(N)_2 + C_5H_8 \qquad (6)$$

2.1.2 Oxidation of Hydrazine

The dinitrogen complexes of manganese containing cyclopentadienyl ligands was prepared by the controlled oxidation of $Mn(\eta^5\text{-}C_5H_5)(CO)_2(N_2H_4)$ with H_2O_2 in the presence of Cu(II) salts at -40°C [Equation (7)] [37].

$$Mn(\eta^5\text{-}C_5H_5)(CO)_2(N_2H_4) + 2\ H_2O_2 \xrightarrow{Cu^{2+}} Mn(\eta^5\text{-}C_5H_5)(CO)_2(N_2) + 4H_2O \qquad (7)$$

The rhenium analogue of the manganese complex has been prepared by the controlled oxidation of $Re(\eta^5\text{-}C_5H_5)(CO)_2(N_2H_4)$ under similar condition [38].

2.1.3 Reduction under Dinitrogen

Most widely used route to dinitrogen complex is the reduction of a complex in the presence of dinitrogen, which forms $\mu\text{-}N_2$ dinuclear complex [Equation (8)] [39].

$$(\eta^5\text{-}C_5H_5)_2TiCl + MeMgI + N_2 \rightarrow \{(\eta^5\text{-}C_5H_5)_2Ti\}_2(N_2) \qquad (8)$$

A dinitrogen complex of bis(pentamethylcyclopentadienyl)zirconium(II) has been prepared by the following sequence [Equation (9)] [40].

$$2(C_5(CH_3)_5)_2ZrCl_2 + 4Na(Hg) + N_2 \rightarrow \{(C_5(CH_3)_5)_2Zr\}_2(N_2)_3 + NaCl \qquad (9)$$

Sometimes the reductant incorporates into the reaction product. The dinitrogen complex $\{[N_3N]MoN_2\}_2Mg(THF)$, ($[N_3N]^{3-} = [Me_3SiNCH_2CH_2]_3N]^{3-}$), for instance, is obtained by the reduction of $[N_3N]MoCl$ by an excess of Mg under dinitrogen [Equation (10)] [41, 42].

$$[N_3N]MoCl + Mg + THF + N_2 \rightarrow \{[N_3N]MoN_2\}_2Mg(THF) + MgCl_2 \qquad (10)$$

All studies were aimed at the reduction of dinitrogen for ammonia production. Theses dinitrogen complexes can neither be produced via dinitrogen adsorption to

preformed complexes, nor reversibly release binding dinitrogens because the reactions involve the replacement of ligands or the transformation of ligands.

2.2 Novel Three-Coordinate Molybdenum(III) Complexes (Cummins Work)

Recently, Cummins and co-workers showed that novel three-coordinate molybdenum(III) complexes $Mo(N[R]Ar)_3$ ($R = C(CD_3)_2CH_3$, $Ar = 3,5\text{-}(CH_3)_2C_6H_3$) have a unique ability to selectively and reversibly absorb N_2 as schematically shown in Figure 2 [25-28]. The formation of N_2 binding complex in hydrocarbon solution under N_2 takes 48 hours at -35°C, while N_2 binding complex is not appreciable at room temperature under these conditions [28]. The more rapid N_2 uptake at -35°C than at room temperature is likely to be a manifestation of the greater solubility of N_2 in organic solvents with decreasing temperature. We expect the solid system provides the more rapid reaction between N_2 atoms and the Mo(III) complex because the rate of the reaction can be controlled by pressure and/or temperature.

The X-ray crystal structure of $Mo(N[R]Ar)_3$ [28] contains a trigonal planar MoN_3 unit with tert-butyl groups and aryl groups located on opposite side of the trigonal plane (Figure 3). The only accessible path to the molybdenum atom even for a small molecule is a pocket surrounded by the three tert-butyl groups.

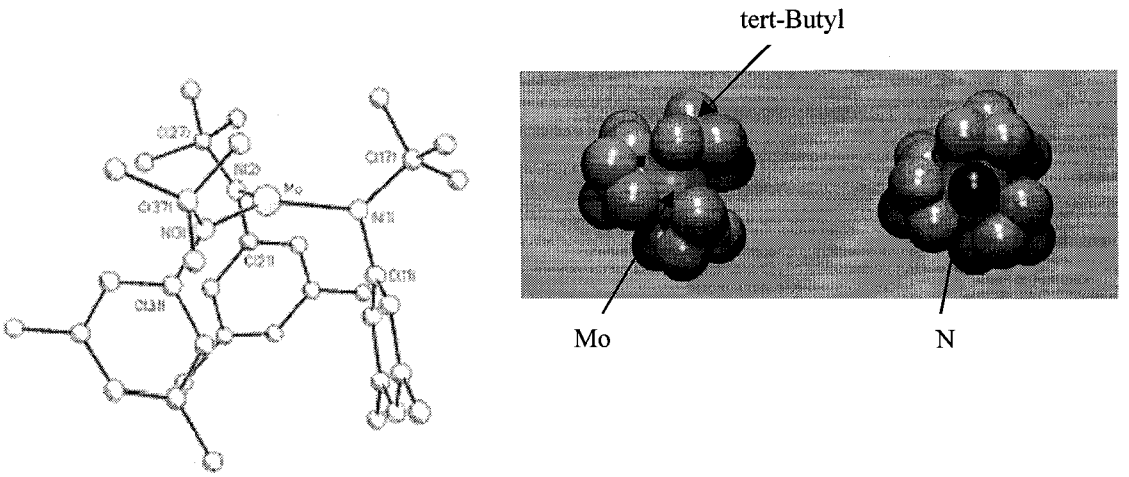

Figure 3. Structural diagram of $Mo(N[R]Ar)_3$ from X-ray coordinates [28].

Molybdenum exhibits all oxidation states between 0 and VI and is more stable in oxidation states VI. In order to provide its active site for dinitrogen, molybdenum should be in a lower oxidation state. The coordination number should be also low to create an empty coordination site for N_2. The choice of the proper ligand is important. Ligands should be large enough so that only small molecules such as N_2 could access the metal center, and avoid β-hydride elimination or cyclometallation reactions. Additionally, the electronic state of substitutes should also be considered. The amido ligand has one alkyl group and one aryl group with a right balance between electron-donating and electron-withdrawing properties, and is bulky enough so that no more than three such ligands can be accommodated around the molybdenum center [27]. Cummins and his co-workers have synthesized Mo(III) complexes with several substitutes and examined the reactivity to dinitrogen. $Mo(N[R]Ph)_3$ (R = tert-butyl, Ph = phenyl) reacts with N_2 in similar manner to $Mo(N[R]Ar)_3$ (Ar = 3,5-dimethylphenyl), that is, it takes 2 days at -35°C to form μ-$N_2[Mo(N[R]Ph)_3]_2$ and the N-N bond splits [27]. Indeed, the X-ray structure of

$Mo(N[R]Ph)_3$ is quite similar in shape to $Mo(N[R]Ar)_3$, thus no special structural significance should be attribute to the aryl methyl substitutions. The mononuclear dinitrogen complex $N_2[Mo(N[R]Ar)_3]$ had not been isolated to verify its structure by X-ray so that the reduction agent, sodium amalgam, was used to trap $N_2[Mo(N[R]Ar)_3]$. However, the obtained $[(THF)_xNa][N_2Mo(N[R]Ar)_3]$ is likely to be dimeric in nature. This particular goal was achieved through the use of more sterically demanding ligand with adamantyl substituents (Ad). When a THF solution of $Mo(N[1\text{-}Ad]Ar)_3$ was stirred over Na/Hg under dinitrogen for 10-35 h at 25°C, the dinitrogen complex $[(THF)_xNa][N_2Mo(N[1\text{-}Ad]Ar)_3]$ was the major product (Figure 4) [43]. Under no conditions has $Mo(N[1\text{-}Ad]Ar)_3$ been observed to split dinitrogen or to transform to a dinuclear complex.

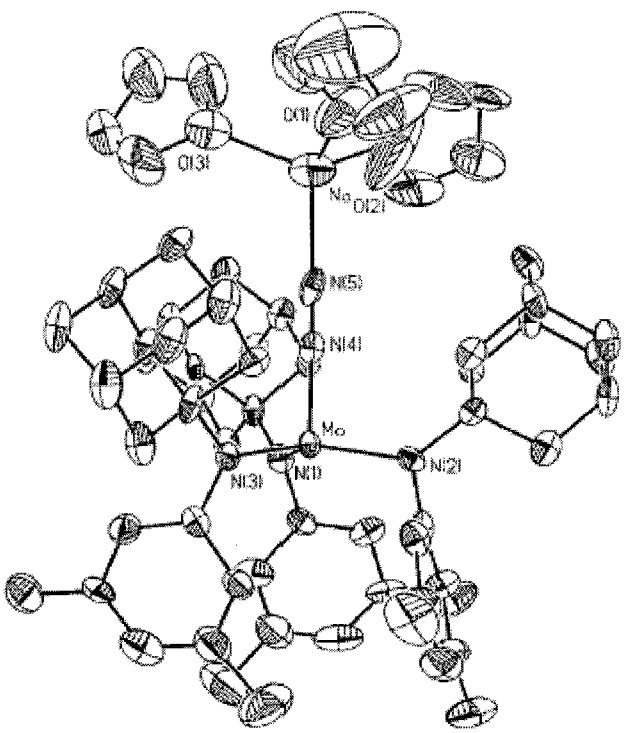

Figure 4. Structural diagram of $[(THF)_xNa][N_2Mo(N[1\text{-}Ad]Ar)_3]$ from X-ray coordinates [43].

Another adamantyl-substituted derivative is $Mo(N[2\text{-}Ad]Ar)_3$ [44]. β-hydrogens in its secondary adamantyl substituents are retained without β-hydrogen elimination, which unlike the attempted synthesis of $Mo(N[i\text{-}Pr]Ar)_3$ (i-Pr = isopropyl) results in the generation of β-hydrogen elimination species $Mo(H)(\eta^2\text{-}Me_2C{=}NAr)N[i\text{-}Pr]Ar)_2$ [45]. The conformational restriction on the motions of the 2-adamantyl groups is probably responsible for the absence of β-hydrogen elimination. The reactivity of $Mo(N[2\text{-}Ad]Ar)_3$ to dinitrogen is similar to $Mo(N[1\text{-}Ad]Ar)_3$.

2.2.1 Formation of the Mo-N_2 Bond

The calculations using the B3LYP method of the density functional theory (DFT) showed that coordination of the N_2 molecule to the Mo(III) complex occurs without an energy barrier to form the complex $(N_2)ML_3$ (L = NH_2) [46, 47]. The N-N distance in $(N_2)ML_3$ is similar to that in free N_2. As to the formation of the Mo-N_2 bond, there are two kinds of important interactions between molybdenum and dinitrogen [48, 49]. One is σ donation from the nitrogen lone pair to an empty orbital of the metal atom and the other is π back-donation from an occupied metal orbital to the empty nitrogen π^* orbital (Figure 5). The molybdenum π-donor orbitals and the nitrogen π^* levels are similar in energy. On the other hand, the lone pair of nitrogen orbital is too low to strongly interact with the empty orbital of the metal. Thus, the main contribution to the Mo-N_2 bond is considered to be the π back-donation.

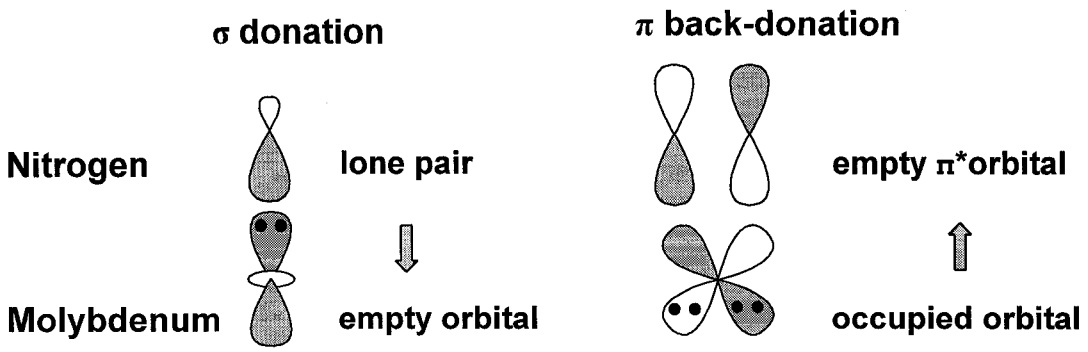

Figure 5. σ donation and π back-donation in the Mo-N_2 bond.

2.2.2 Selectivity for Nitrogen over Carbon Dioxide

No observable reaction between $Mo(N[R]Ar)_3$ and CO_2 (either 1 equiv or 10 equiv, at 1 atm) was reported at 25 °C in a sealed reaction vessel [50]. CO_2 is potential oxo donor for $Mo(N[R]Ar)_3$ because oxygen atoms have lone pairs to coordinate to Mo(III) complexes. If the Mo-O bonds were thermodynamically unstable, this might explain the observed selectivity. In order to investigate this further, the Mo-O bond dissociation enthalpy was determined experimentally using the reaction of pyridine *N*-oxide with Mo(III) complex by solution calorimetry [Equation (11)] [50].

$$Mo(O)(N[R]Ar)_3 \rightarrow [O] + Mo(N[R]Ar)_3 \qquad (11)$$

$\Delta H_{rxn} = 155.6 \pm 1.6$ kcal mol^{-1}

This result shows the Mo-O bond is one of the strongest known transition metal-oxygen bonds. Moreover, the enthalpy of reaction $Mo(N[R]Ar)_3$ with CO_2 was calculated to be thermodynamically downhill by about 30kcal/mol. Therefore, the observed selectivity cannot be explained by the instability of $Mo(O)(N[R]Ar)_3$. The overlap populations and net atomic charges for $Mo(O)(N[R]Ar)_3$ and $Mo(N)(N[R]Ar)_3$ were estimated by

extended the Hückel methodology [50]. The value of the overlap population indicates the degree of matching between two atoms in term of orbital energies and radial properties for interaction. The overlap populations are as follows: Mo-O 0.67; Mo-$N_{nitrido}$ 1.11. Summing of the charges in the orbitals associated with each atom gives the net atomic charge. The larger the difference in the value of nets atomic charge between two bonded atoms, the greater the ionic bond property. The net atomic charges are: Mo, O (+2.640, -1.417); Mo, $N_{nitrido}$ (+3.028, -1.863). These results show that Mo-N has greater overlap population and is characterized more by an ionic bond than in the case of Mo-O. Although no further studies of the reaction $Mo(N[R]Ar)_3$ with CO_2 were performed and the cause of inactivity of the Mo(III) complex to CO_2 has not been elucidated, the affinity of these unique complexes to N_2 prompted us to utilize the Mo(III) complexes for selective removal of nitrogen from flue gas laden with CO_2, acid gas impurities and water.

2.2.3 Reaction of $Mo([R]Ar)_3$ with other gas impurities, NO_2, NO and SO_2 in flue gas

$Mo([R]Ar)_3$ in diethylether at 25 °C was treated with 0.5 equivalent gaseous NO_2, resulting in a rapid color change to brown over 10 min [Equation (12)] [50]. ^1H and ^2H-NMR spectroscopy analysis of the reaction mixture confirmed the presence of oxo $Mo(O)([R]Ar)_3$ and the known terminal nitrosyl complex $Mo(NO)(N[R]Ar)_3$. $Mo([R]Ar)_3$ had been completely consumed.

$$2Mo([R]Ar)_3 \xrightarrow{NO_2} O{=}N{=}Mo([R]Ar)_3 + O{=}Mo([R]Ar)_3 \qquad (12)$$

Bubbling of nitric oxide through diethylether containing $Mo([R]Ar)_3$ immediately gave the nitrosyl complex $Mo(NO)(N[R]Ar)_3$ [Equation (13)] [26].

$$Mo([R]Ar)_3 \xrightarrow{NO} O{=}N{=}Mo([R]Ar)_3 \qquad (13)$$

$Mo([R]Ar)_3$ removes one oxygen from SO_2 [Equation (14)]. Treatment of ethereal $Mo([R]Ar)_3$ with 0.6 equivalent of gaseous SO_2 led to an immediate color change to dark brown [50]. Analysis of the reaction mixture confirmed complete conversion of $Mo([R]Ar)_3$ to oxo $Mo(O)([R]Ar)_3$ and sulfide $Mo(S)([R]Ar)_3$ in a 2:1 ratio as determined by ^{2}H-NMR spectroscopy.

$$3Mo([R]Ar)_3 \xrightarrow{SO_2} S{\equiv}Mo([R]Ar)_3 + 2O{=}Mo([R]Ar)_3 \qquad (14)$$

$Mo([R]Ar)_3$ readily reacts with NO_2, NO and SO_2. For the application of this complex to separate N_2 from flue gas in the presence of NO_2, NO and SO_2, an SCR unit for NO_x removal and a wet scrubber for the SO_x removal may need to be deployed before the N_2/CO_2 separation membrane.

2.2.4 Selection of Substituents for Amido Ligands

The literature review indicated that every two $Mo(N[R]Ar)_3$ complexes bind one nitrogen molecule because they form so-called dinuclear μ-N_2 complexes [43], i.e. Mo-N=N-Mo, which results in a decreased capacity of this material as well as undesirable N-N bond splitting (Figure 6). The same literature review further indicated that this undesirable dimerization may be avoided by using $Mo(N[1\text{-}Ad]Ar)_3$ complex containing bulky adamantyl groups (Ad) instead of smaller *t*-butyl (*t*-Bu) as shown in Figure 7.

Because of the size of the Ad group, the Mo atom of the second complex cannot approach the uncoordinated end of the nitrogen molecule already bound to a Mo complex.

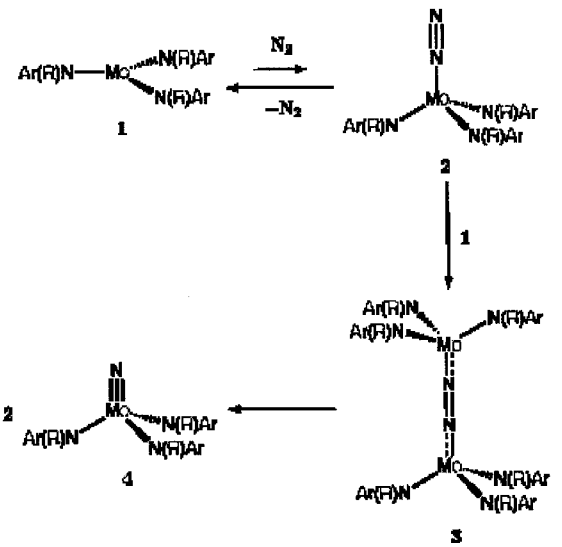

Figure 6. Formation of dinuclear μ-N_2 complexes and splitting of dinitrgen [43].

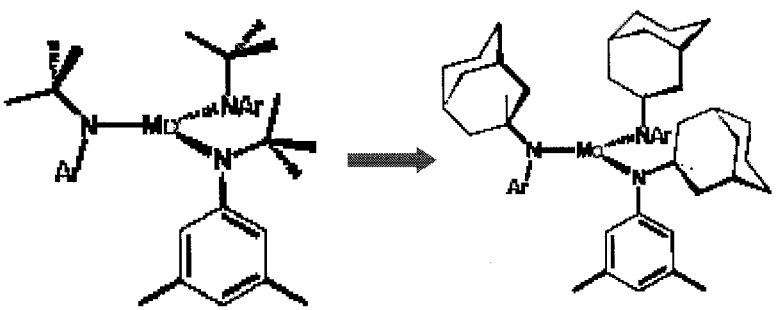

Figure 7. Three-coordinate Mo(III) complexes with t-butyl (left) and 1-adamantyl (right) ligands.

Chapter 3

Plan to Achieve Research

The Mo(III) complex with high affinity to reversible N_2 chemisorption does not appear to bind CO_2; however, effect of impurities and stability have not been investigated. The goals of this research is to synthesize three-coordinate Mo(III) complexes, to investigate the N_2 separation ability from CO_2 and other gas impurities, and to examine the stability of these unique N_2-binding complexes for the practical application.

3.1 Synthesis and Characterization of Mo(III) Complexes

Three-coordinate Mo(III) complexes with bulky substitutes, $Mo(N[1\text{-}Ad]Ar)_3$ (Ad = adamantyl, Ar = 3,5- $(CH_3)_2C_6H_3$) will be synthesized according to published 6-step synthesis procedure (Figure 8). All intermediate compounds required, namely *N*-1-adamantyl-3,5-dimethylaniline ligand (step 1), the intermediate $Li(N[1\text{-}Ad]Ar)(OEt_2)$ complex in step 2, and the intermediate $MoCl_3(THF)_3$ complex in steps 3-5 will be characterized by ^{1}H-NMR or/and GC/MS. The final product, three-coordinate Mo(III) complex $Mo(N[1\text{-}Ad]Ar)_3$ will be identified by the measurement of TOF/MS and a powder X-ray diffraction pattern.

Step 1

$$ArNH_2 + BrAd \rightarrow HN[1\text{-}Ad]Ar + HBr$$

Step 2

$$HN[1\text{-}Ad]Ar + MeLi + Et_2O \rightarrow Li(N[1\text{-}Ad]Ar)(OEt_2) + CH_4$$

Step 3

$$MoCl_5 + excess CH_3CN \rightarrow MoCl_4(CH_3CN)_2 + \text{chlorinated organics}$$

Step 4

$$MoCl_4(CH_3CN)_2 + excessTHF \rightarrow MoCl_4(THF)_2 + 2CH_3CN$$

Step 5

$$MoCl_4(THF)_2 + excessTHF \xrightarrow[CH_2Cl_2]{Zn} MoCl_3(THF)_3$$

Step 6

$$MoCl_3(THF)_3 + 3Li(N[1\text{-}Ad]Ar)(OEt_2) \xrightarrow[Et_2O]{} Mo(N[1\text{-}Ad]Ar)_3 + 3LiCl$$

Figure 8. Synthesis of three-cordinate Mo(III) complexes

3.2 Investigation of N_2 Chemisorption and Separation from Flue Gas Impurities on Three-Coordinate Mo(III) Complexes

Single-component adsorption and desorption of N_2, CO_2, and other gas impurities, e.g. SO_2, H_2O, NO, and NO_2, will be investigated at 50-160 °C and P= 0.1-10 atm employing a Cahn adsorption microbalance. In these experiments we will also determine the gravimetric uptake rate (both adsorption and desorption) of these various species, which is critical for the development of commercial separation process. The performance of these complexes will be evaluated with respect to (i) adsorption rate, (ii) equilibrium sorption capacity, and (iii) separation selectivity, which will be determined by a GC/MS analysis of the gas phase at equilibrium.

3.3 Determination of Stability of N_2-binding Complexes for the Practical Application.

The effect of water, SO_x, and NO_x on the N_2/CO_2 separation selectivity and N_2 sorption capacity will be investigated by subjecting three-coordinate Mo(III) complexes to a long-term exposure (up to 2 months) to these impurities (50-3000 ppm levels for SO_x, and NO_x, 5-20% for water vapor) followed by collection of N_2 adsorption data using a Cahn adsorption microbalance. We will also examine the thermal stability of the three-coordinate Mo(III) complexes in TGA experiments, which are expected to be stable at least up to their melting point temperature of ~200°C.

Chapter 4

Experimental Procedure and Results

4.1 High Performance Glove Box

A high-performance glove box is required for intermediate synthesis steps 2-6 in Figure 8 because of the sensitivity of synthesis to moisture and oxygen. Such a glove box has been identified in the organic synthesis laboratory in the chemistry department at the University of Cincinnati. The glove box has an evacuable chamber (ante-chamber) used for passing materials in and out without disturbing the glove box atmosphere. Anytime the ante-chamber was exposed to atmosphere, the air in the ant-chamber is completely evacuated and refilled with argon and this evacuation/refill process is repeated for at least 3 times. An automatic pressure controller of the glove box can adjust pressure inside the box automatically by removing inert gas or adding inert gas. Moreover, the high performance glove box maintains a moisture and oxygen-free environment by self-purification. Inert gas in the box is continuously cycle through a purifier which removes moisture and oxygen contamination from any source (Figure 9), such as:

1. Diffusion through the rubber gloves in the glove box.
2. Insertion of contaminated parts into the glove box.
3. Use of makeup gas which is not completely free of moisture or oxygen.

The purifier contains two chemical agents. One is a molecular sieve which removes moisture from gas flowing through it by a process of molecular adsorption. The other agent is an oxygen getter, copper on an alumina matrix. When one of the agents in the purifier becomes saturated with oxygen or moisture, it should be regenerated. The regeneration procedure starts with 3 hours heating process at 200°C to boil off moisture, and then 1 hour purging process with hydrogen mixture gas to remove trapped oxygen,

followed by 8 hours vacuuming process to remove water generated during purging process.

This glove box has not been in use for a considerable period of time, so that air leaks and electrical problems in the system were needed to be fixed. To restore the glove box, the following procedure was conducted.

1. Cleaning inside.
2. Replacement of gloves and its o-rings (o-rings were badly damaged.)
3. Adjustment the position of a chamber door inside. (It was not open and close properly because of the malposition.)
4. Leakage-check of the glove box. (No leakage.)
5. Set-up a new vent line and connected hydrogen cylinder with the regenerator.
6. Power on. (It did not work because one contactor in the controller was not closed. Pushing the reset switch on the front face of the safety controller and the start switch on the 220V breaker box behind the controller at the same time is required to start up.)
7. Line leakage check. (2 nuts were loose. One was in argon line between the controller and the glove box and the other was in another argon line directly connected to the glove box from argon cylinder.)
8. Established an inert atmosphere in the glove box.
9. Regeneration of the purifier 4 times.
10. Circulation of argon through the purifier.
11. Vacuum pump oil change.

After the repair, the glove box was checked routinely by $TiCl_4$ and $Zn(C_2H_5)_2$ test and maintained the condition of oxygen < 5ppm and water < 10ppm.

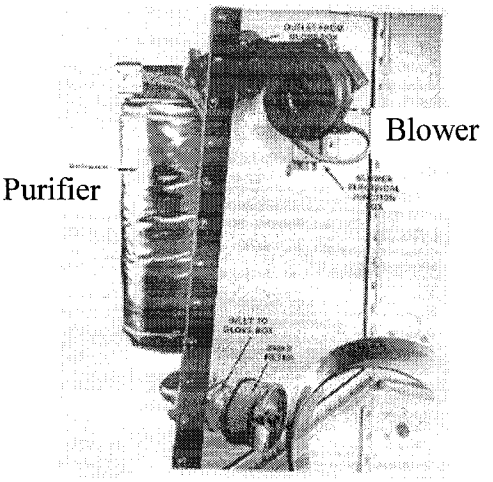

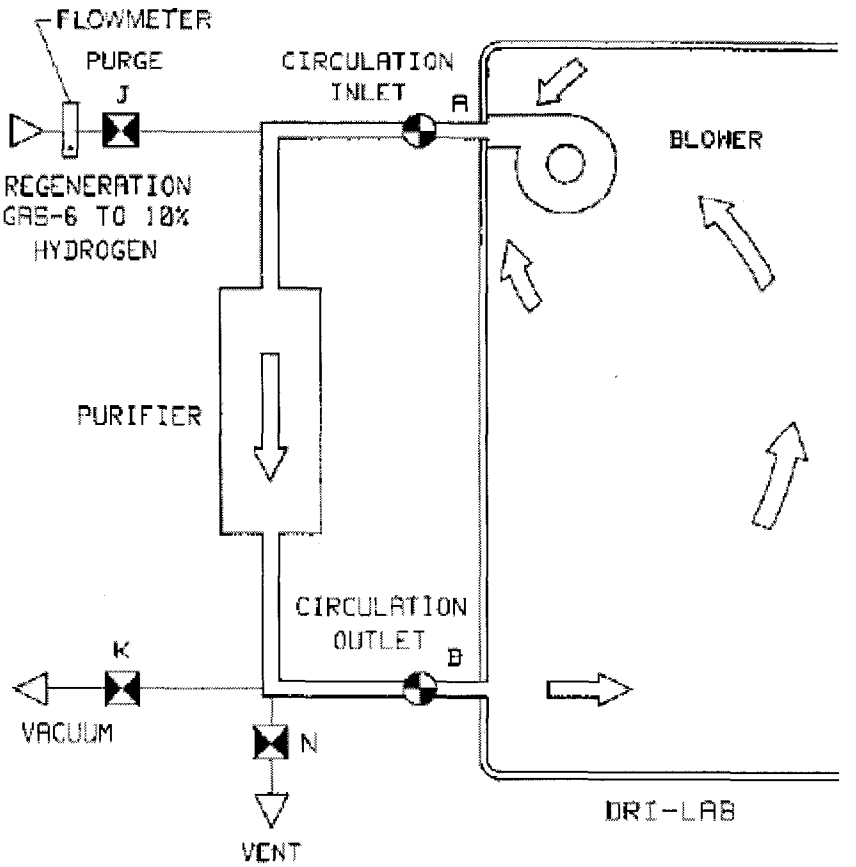

Figure 9. Diagram of high performance glove box.

4.2 Synthesis and Characterization of HN[1-Ad]Ar (Step 1)

N-1-adamantyl-3,5-dimethylaniline (HN[1-Ad]Ar) is the ligand used in the synthesis of the target Mo(III) complex. 11 papers have been published on synthesis of HN[1-Ad]Ar, 6 of them are Cummins's work [51] at MIT and 5 of them are Rheingold's work [52] at University of Ottawa. There are only two general synthesis methods and each group's method is different from that of the other. The Cummins method is based on the published synthesis procedure of *N*-1-adamantylaniline by Watts *et al.* [53]. The Watts method needs about 5 equivalent of aniline to be added to 1 equivalent of 1-bromoadamantane, with the excess aniline producing *N*-bromoaniline as a side product [Equation (15)]. The separation of *N*-bromoaniline from *N*-1-adamantylaniline in the presence of excess aniline is somewhat problematic.

$$5ArNH_2 + BrAd \rightarrow HN[1\text{-}Ad]Ar + ArNH_3Br + 3ArNH_2 \qquad (15)$$

On the other hand, Rheingold at University of Ottawa made a modification of the Watts procedure. His method requires 1 equivalent of 3,5-dimethylaniline per 1 equivalent of 1-bromoadamantane, and the *N*-bromo-3,5-dimethylaniline by-product is not formed [Equation (16)].

$$ArNH_2 + BrAd \rightarrow HN[1\text{-}Ad]Ar + HBr \qquad (16)$$

Synthesis trials by both methods have been conducted and HN[1-Ad]Ar was successfully obtained each time. Although the Rheingold synthesis method is simpler, it resulted in a lower yield of HN[1-Ad]Ar because of the solidification of the synthesis medium which prevented effective reagent mixing. According to the Cummins method, the product was obtained in slightly higher yield (50%). However, the product purification procedure was more complicated and required 4-5 days to complete. Thus, a

modified synthesis procedure was developed based on the technique described by Rheingold *et al.* In our modified method, the ratio of 3,5-dimethylaniline and 1-bromoadamantane was 2:1[Equation (17)].

$$2ArNH_2 + BrAd \rightarrow HN[1\text{-}Ad]Ar + ArNH_3Br \qquad (17)$$

The excess 3,5-dimethylaniline was expected to help mixing at the early stage of the reaction and to be completely consumed due to formation of *N*-bromo-3,5-dimethylaniline. HN[1-Ad]Ar was obtained reproducibly in yield ranging 95-96% with >99.9% purity. The results of a series of synthesis runs are summarized in Table 2.

	Run1	Run2	Run3	Run4
Method	Rheingold	Cummins	Modified	Modified
Aniline : BrAd	1 : 1	5 : 1	2 : 1	2 : 1
Temprature	165°C	140℃	165℃	165℃
Reaction Time	4h	25h	4h	4h
Isolation Time	1.5 days	4-5 days	1.5 days	1.5 days
Yield	7.45g, 41%	10.35g, 50%	20.07g, 96%	19.87g, 95%

Table 2. Synthesis of HN[1-Ad]Ar using different methods.

4.2.1 Experimental Procedure

$CHCl_3$ was purchased from Acros; MeOH was from Pharmco; 1-bromoadamantane and 3,5-dimethylaniline were purchased from Aldrich; NaOH, anhydrous $MgSO_4$ and Et_2O were from Fisher; $CDCl_3$ was from Cambridge Isotope Laboratories. All solvents and reagents were used without purification.

4.2.1.1 The synthesis of HN[1-Ad]Ar by Rheingold method [52]

In a 100-ml, round-bottom flask equipped with magnetic stir bar, 1-bromoadamantane (15.50 g, 72 mmol) was dissolved in 3,5-dimethylaniline (8.70 g, 72

mmol) yielding a clear, pale yellow solution. This solution was heated under nitrogen for 4 h at 165°C to form a brown solid. The brown solid was grounded and washed with a minimum volume of Et_2O and then, treated with NaOH (40 ml of a 10% solution). The mixture was extracted with 3 portions of CH_2Cl_2, and the organic phase was washed with water and dried over $MgSO_4$ overnight. After filtration, the solvent was removed in vacuo, yielding HN[1-Ad]Ar (7.45 g, 29 mmol, 40% yield) as a white microcrystalline solid.

4.2.1.2 The synthesis of HN[1-Ad]Ar by Cummins method [51]

In a 100-ml, round-bottom flask equipped with magnetic stir bar, 1-bromoadamantane (17.50 g, 80 mmol) was dissolved in 3,5-dimethylaniline (46.00 g, 380 mmol) yielding a clear, pale yellow solution. This solution was heated under nitrogen for 24-36 h at 140°C to form a thick brown liquid. The brown liquid was mixed with Et_2O (100 ml), washed with NaOH (50 ml of a 1 M solution), and vacuum distilled to remove excess 3,5-dimethylaniline leaving a dark brown solid. The solid was dissolved into a minimum volume of hot methanol (50 ml) and cooled until crystallization occurred. The solid was collected on a sintered-glass frit and washed with cold methanol (2 × 10 ml) to afford white crystals (10.35 g, 40 mmol, 50% yield).

4.2.1.3 Modified procedure of Tsunakawa

In a 100-ml, round-bottom flask equipped with magnetic stir bar, 1-bromoadamantane (17.50 g, 81 mmol) was dissolved in 3,5-dimethylaniline (19.50 g, 160

mmol) yielding a clear, pale yellow solution. This solution was heated under nitrogen for 4 h at 165°C to form a brown solid. The brown solid was grounded and washed with a minimum volume of Et_2O, treated with NaOH (50 ml of a 10% solution). The mixture was extracted with 2 portions of CH_2Cl_2, and the organic phase was washed with 2 portions of water and dried over $MgSO_4$ overnight. After filtration, the solvent was removed in vacuo, yielding HN[1-Ad]Ar (20.01 g, 78 mmol, 96% yield) as a white microcrystalline solid.

4.2.2 Physicochemical Characterization of HN[1-Ad]Ar

^{1}H-NMR spectra were recorded on a Bruker AC 250 spectrometer. The peak positions were reported with positive shifts in ppm downfield of tetramethylsilane (TMS). GC/MS measurements were carried out on a HP5980.

A single peak at retention time 16.11 min was obtained in Total Ion Chromatography (TIC) from GC/MS (Figure 10). This result indicates that the purity of the sample is >99.9%. The mass spectrum of this peak is shown in Figure 11. The base peak (the largest peak) was m/z 198 and the parent ion was m/z 255, which corresponded to the mass of HN[1-Ad]Ar. The m/z 135 and 105 could be assigned to an adamantyl group and a 3,5-dimethylbenzyl group, respectively. Peaks in ^{1}H-NMR spectrum were also well consistent with the structure of HN[1-Ad]Ar and no extra peaks were observed (Figure 12). Consequently, the synthesized material was identified as HN[1-Ad]Ar.

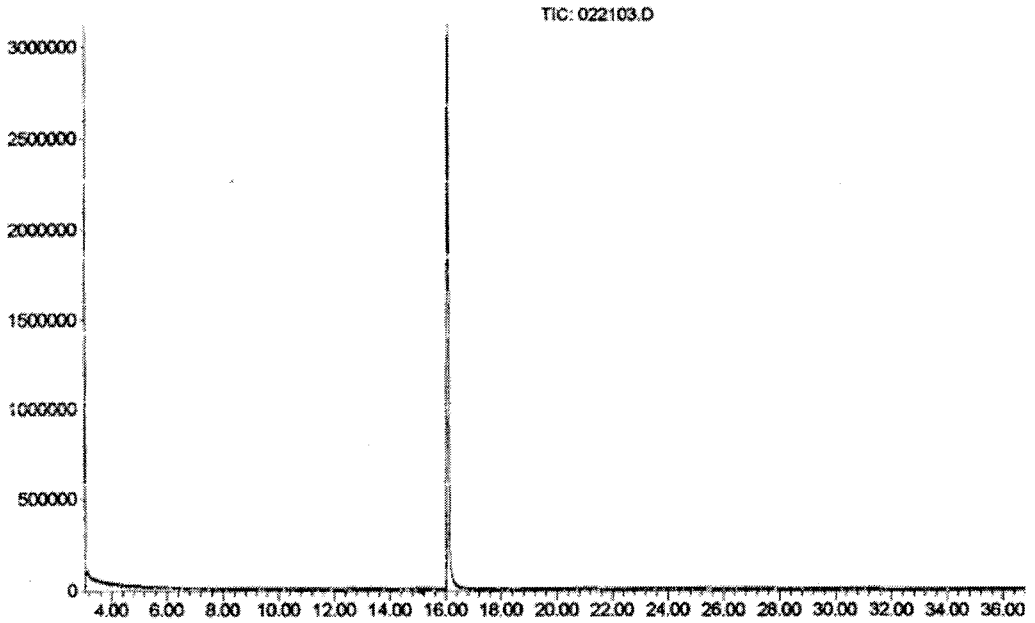

Figure 10. TIC of GC-MS analysis of pure HN[1-Ad]Ar.

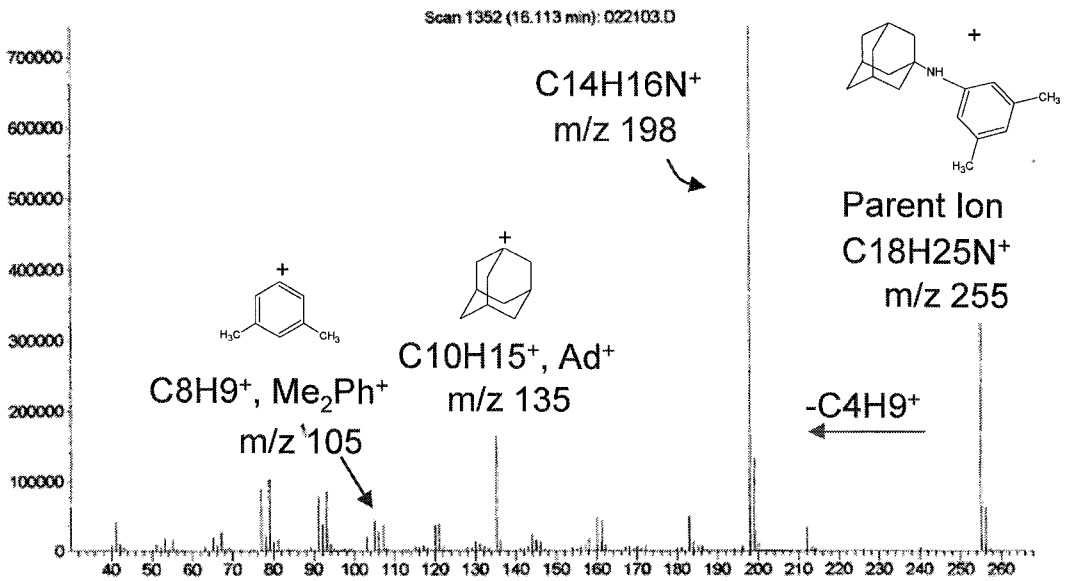

Figure 11. Mass Spectrum of HN[1-Ad]Ar. MS (70eV, %), m/z 255 (M+, 46), 198 (base).

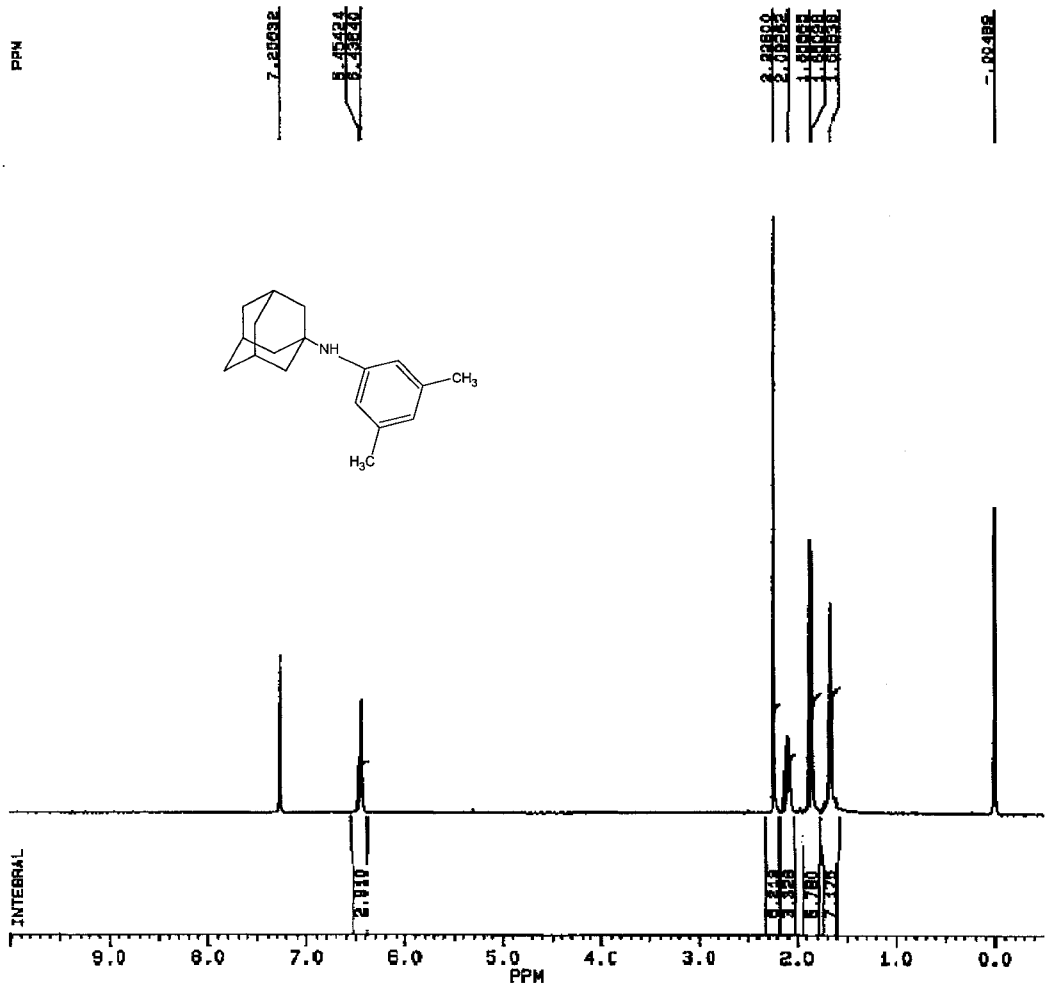

Figure 12. ^{1}H-NMR (250MHz, $CDCl_3$) of HN[1-Ad]Ar.

δ= 6.45 (s,1H), 6.44 (S, 2H, aryl), 2.23 (s, 6H, aryl$(CH_3)_2$), 2.09 (s, 3H, adamantyl methine), 1.85 (d, 6H, adamantyl crown methylene), 1.66 (s, 6H, adamantyl methylene)

4.3 Synthesis and Characterization of Li(N[1-Ad]Ar)(OEt_2) (Step 2)

Lithium *N*-1-adamantyl-3,5-dimethylaniline etherate, Li(N[1-Ad]Ar)(OEt_2) was prepared according to the published method in a 89 % yield [52]. However, Li(N[1-Ad]Ar)(OEt_2) was air- and moisture- sensitive. Thus, it had to be prepared just before its use in further synthesis steps.

4.3.1 Experimental Procedure

C_6D_6 and MeLi were purchased from Aldrich, and anhydrous Et_2O was purchased from Fisher. A solution of HN[1-Ad]Ar (6.39g, 25 mmol) in argon-sparged Et_2O (125ml) is frozen in liquid nitrogen and allowed to thaw until magnetic stirring was just possible. A solution of MeLi (16 ml, 1.6M in Et_2O, 26 mmol) was slowly added by a syringe over 5 min period. The reaction mixture was allowed to warm to room temperature while a white solid precipitated. After 3 h stirring at room temperature, the product was collected by filtration and dried under vacuum. Yield 7.50 g (89%).

4.3.2 Physicochemical Characterization of Li(N[1-Ad]Ar)(OEt_2)

The synthesized white precipitate was measured by a Bruker AC 250 ^{1}H-NMR spectrometer. The peak positions were reported with positive shifts in ppm downfield of tetramethylsilane (TMS). The deuterobenzene used as solvent for the measurement was degassed and dried over activated molecular sieves (4Å). Obtained chemical shifts were assigned to as follows: δ = 6.55 (s, 1H, aryl), 6.51 (s, 2H, aryl), 3.30 (q, 4H, Et_2O), 2.25 (broad, 6H, aryl(CH_3)$_2$), 1.97 (broad, 3H, adamantyl methine), 1.86 (broad, 6H,

adamantyl crown methylene), 1.55 (s, 6H, adamantyl methylene), and 1.14 (t, 6H, Et_2O) [52] (Figure 13).

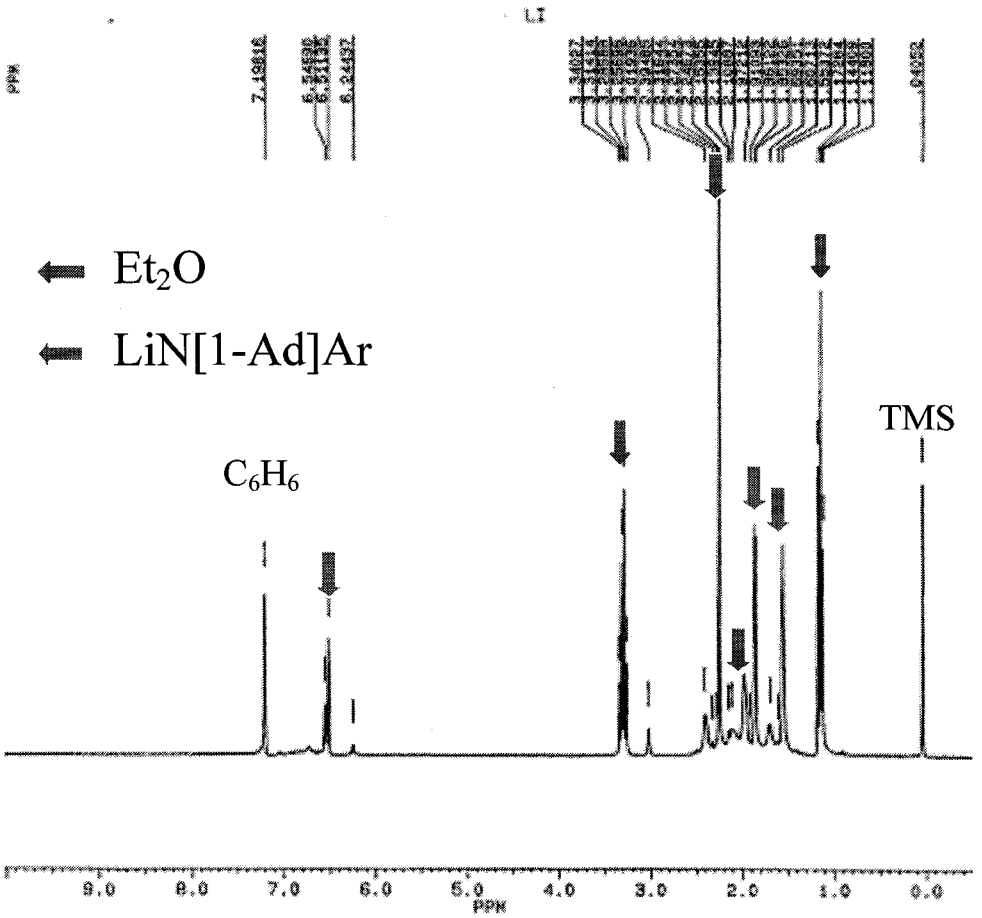

Figure 13. ^{1}H-NMR (250MHz, C_6D_6) of Li(N[1-Ad]Ar)(OEt_2).

4.4 Synthesis and Characterization of $MoCl_3(THF)_3$

$MoCl_5$ is commercially available Mo-containing starting material. This pentachloride compound is a strong Lewis acid and also a powerful oxidant and its direct reduction in THF results in the acid-catalyzed ring opening polymerization of THF, which may be avoided by replacing THF with other solvents. The most commonly used

synthesis method consists of 3 steps [54]: (i) the reaction of $MoCl_5$ with acetonitrile CH_3CN to afford $MoCl_4(CH_3CN)_2$; (ii) the replacement of the nitrile with THF; (iii) the reduction of $MoCl_4(THF)_2$ to $MoCl_3(THF)_3$. This original 3-step method for making this compound shown in Figure 8 was unsuccessful. We obtained brownish-orange solution instead of the blue clear solution. The brownish-orange color might be the result of the formation of the dinuclear complex, $Mo_2Cl_6(THF)_3$. As will be discussed ^{1}H-NMR study in section 4.4.2 that the $MoCl_3(THF)_3$ readily transforms to the dinuclear complex in CD_2Cl_2. To avoid the formation of the dinuclear complex, CH_2Cl_2 should not be used for the synthesis. We have identified a one-step alternative approach shown in Figure 14, which does not involve the use of CH_2Cl_2. [55]. In this alternative method, Mo(V) pentachloride is reduced by elemental tin first in Et_2O and then in tetrahydrofuran (THF) after Et_2O is replaced with THF by decanting. The pale orange-brown $MoCl_3(THF)_3$ complex was obtained at 77 % yield by this method.

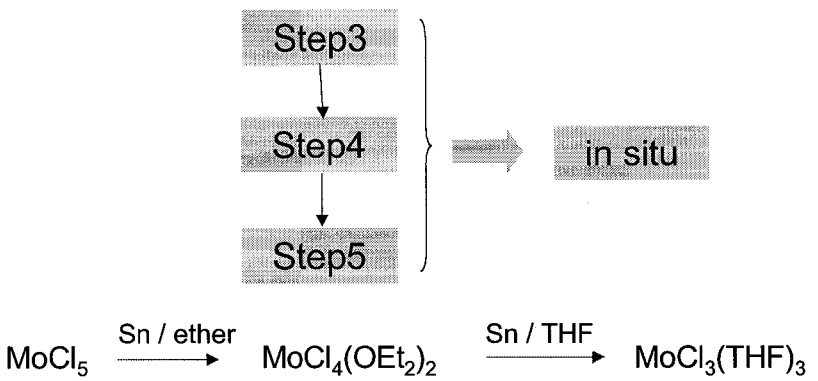

Figure 14. One-step synthesis of $MoCl_3(THF)_3$.

4.4.1 Experimental Procedure

All operations were performed in a glove box under an atmosphere of purified argon. Anhydrous CH_2Cl_2 was purchased from Acros; THF was from Pharmco; $MoCl_5$ was purchased from Aldrich; zinc shot, tin shot, acetonitrile and anhydrous Et_2O were from Fisher. Acetonitrile distilled from CaH_2 under argon. Zinc shot and tin shot were activated in vacuo overnight at a temperature above 180°C. THF was distilled from metal sodium under argon. Anhydrous Et_2O was sparged with argon.

4.4.1.1 Synthesis of $MoCl_4(CH_3CN)_2$ (Step 3) [54]

$MoCl_5$ (25.00 g, 92 mmol) was added slowly over 0.5 h to stirred 125 ml of acetonitrile. The resulting suspension was stirred for a further 2 h and was then allowed to stand at room temperature overnight. The product was filtered and washed with acetonitrile. A fine orange-brown powder was collected on a frit and dried in vacuo. Yield 23.24 g (79%).

4.4.1.2 Synthesis of $MoCl_4(THF)_2$ (Step 4) [54]

Tetrahydrofuran (THF) (90 ml) was added to $MoCl_4(CH_3CN)_2$ (22.50g, 70 mmol) in a flask and the mixture was stirred rapidly for 2 h to give a yellow suspension. The product was filtered and washed with THF. A fine orange-yellow powder was collected on a frit and dried in vacuo. Yield: 7.20 g (27%).

4.4.1.3 Attempted synthesis of $MoCl_3(THF)_3$ (Step 5) [54]

$MoCl_4(THF)_2$ (7.20g, 19 mmol) and zinc shot (12.00g, 183 mmol) were added in the mixture of 36 ml of CH_2Cl_2 and 24ml of THF. The solution was stirred at 0°C for overnight. The orange-brown solution was obtained instead of the blue clear solution. The solution was filtered cold to remove the excess zinc and then evaporated. THF (12 ml) was added to the residue in a flask. No precipitate was obtained.

4.4.1.4 Synthesis of $MoCl_3(THF)_3$ (in situ) [55]

$MoCl_5$ (3.18 g, 11.64 mmol) and coarse tin powder (2.77 g, 23.33 mmol) were suspended in 30 ml of Et_2O. The mixture was then stirred for 2 h at room temperature to form an orange solution and orange solid. The supernatant liquid was decanted off and 30 ml of THF was added. The mixture was then stirred at room temperature overnight. Under gentle stirring with a magnetic stirring bar, the metallic tin remained at the bottom of the flask and supernatant suspension of $MoCl_3(THF)_3$ was transferred into a new flask The pale orange-brown crystalline product $MoCl_3(THF)_3$ was then washed with Et_2O (2 × 15 ml) and dried under vacuum. Yeild: 3.74 g (77%).

4.4.2 Physicochemical Characterization of $MoCl_3(THF)_3$

Identification of $MoCl_3(THF)_3$ was not simple because of its paramagnetism and instability. The ^{1}H-NMR spectrum of $MoCl_3(THF)_3$ in CD_2Cl_2 solution changes with time due to dimerization. The dimerized structures are illustrated in Figure 15. The characteristic paramagnetic shifts of Compound I were obtained at 50-70ppm by widening the measurement window from 15ppm to 70ppm (Figure 16). Compound II was not observed in our result. According to the Poli's report [56], the dimer II initially

increases to a maximum of 19 % of the total Mo concentration after 6 min at 30°C but subsequently disappears, and Compounds III and IV increase in concentration throughout the experiment, as does free THF. Since our sample was measured about 30 min after the preparation, the obtained result was consistent with the reported result.

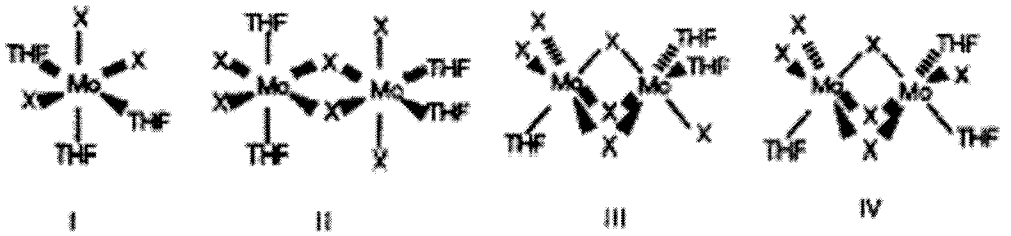

Figure 15. Structures change of $MoCl_3(THF)_3$ in CD_2Cl_2 (X=Cl) [56].

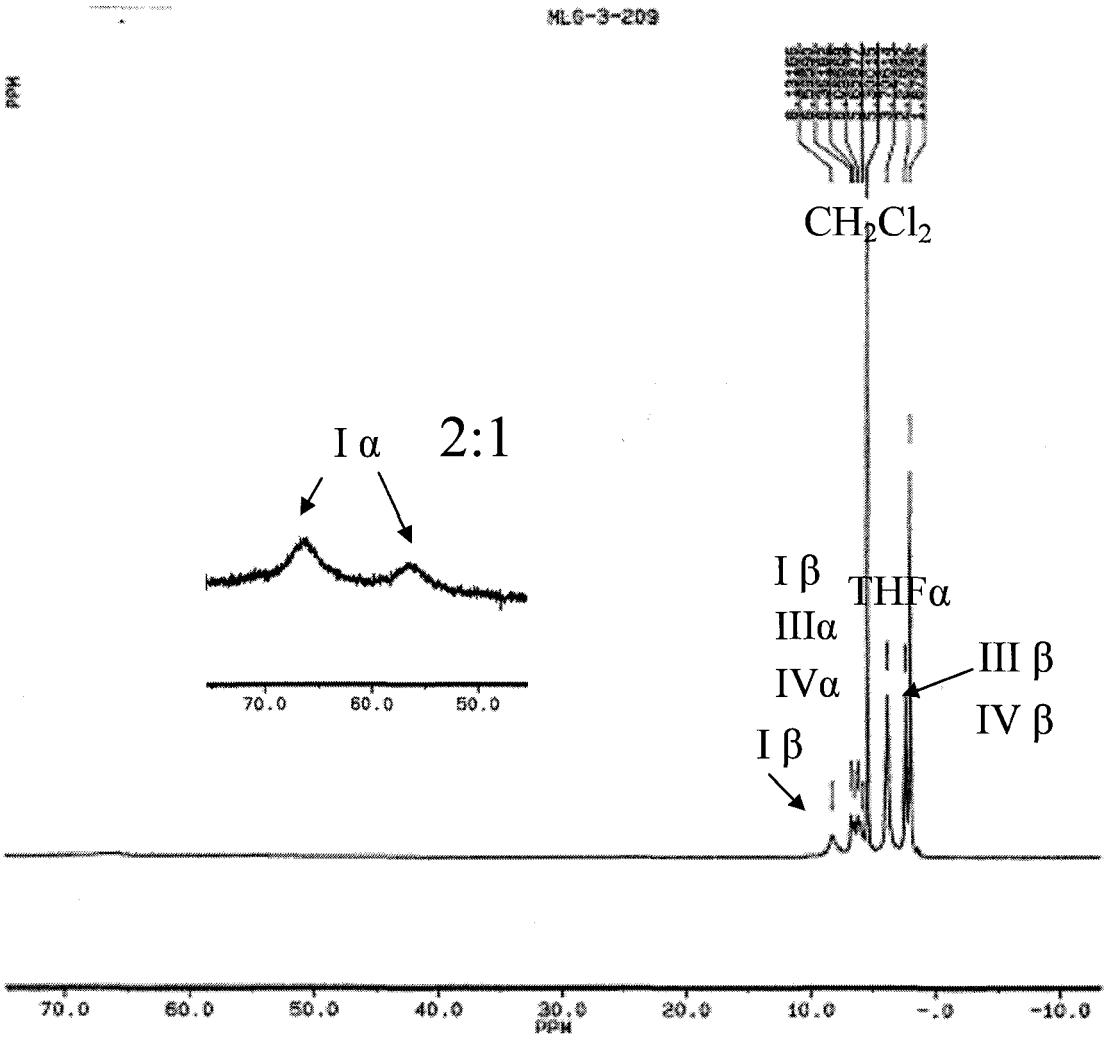

Figure 16. Identification of $MoCl_3(THF)_3$ by ^{1}H-NMR.

4.5 Synthesis and Characterization of Mo(N[1-Ad]Ar)$_3$ (Step 6) [43]

Several synthesis trials were carried out, however, the target Mo(III) complex was not obtained. The reason was that the cooling of the synthesis solution had to be carried out outside of low oxygen and moisture glove box for the lack of a cooling apparatus inside the glove box, which resulted in undesirable oxidation of the product. Cooling apparatuses used outside glove box are shown in Figure 17 and 18. In method A, the

flask covered with plastic bags filled with argon gas was kept in a refrigerator. This method could not prevent oxidation of the product during cooling.

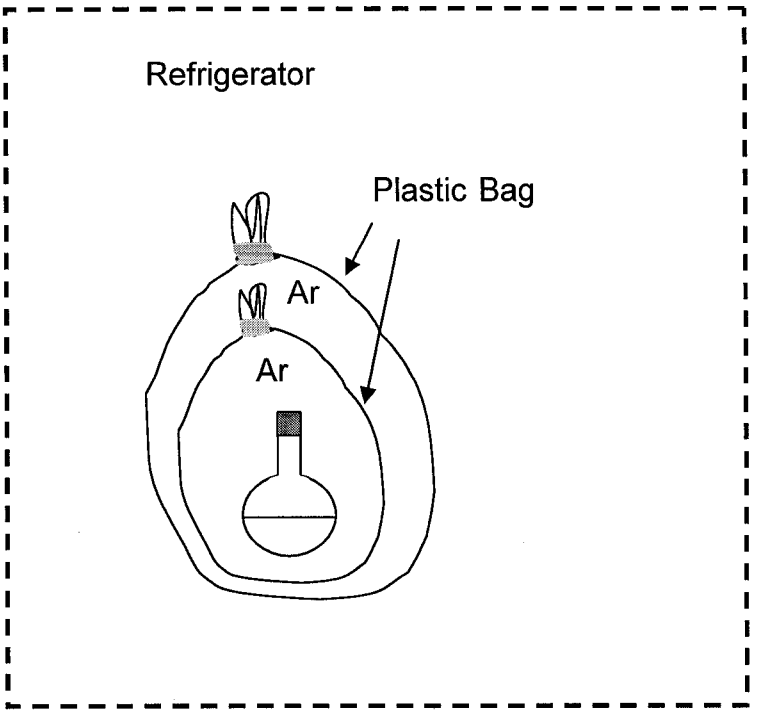

Figure 17. Cooling apparatuses used outside glove box (method A).

In method B, the flask was placed in an isopropanol bath and temperature is manually adjusted by adding dry ice. In order to maintain inert atmosphere inside the flask, argon gas passed through the flask. The product was not oxidized during cooling but the cold flask cools the air around the glass and generates clinging water drops outside the flask glass. This water drops was not able to be removed when the flask was replaced into the glove box for cold filtering. As a result, the product was oxidized during filtration.

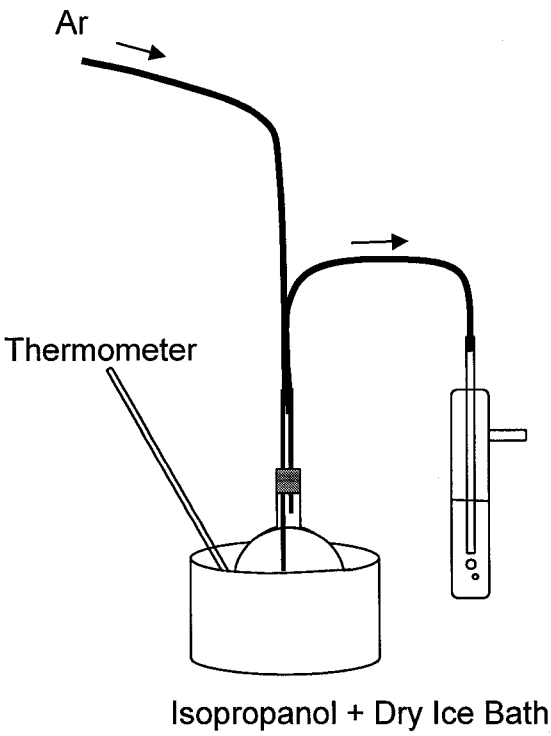

Figure 18. Cooling apparatuses used outside glove box (method B).

Therefore, a cooling system in a glove box was necessary to perform the synthesis in moisture and oxygen free atmosphere. The cooling system developed is shown in Figure 19. The concept of this system is to cool a flask by circulating chilled nitrogen gas through a tube. The system has two cupper tube coils. The one outside the glove box is place into liquid nitrogen and nitrogen gas is passed through it to cool the second coil located inside the glove box. We attempted to chill diethyl ether in a round bottom flask. The first trial, the temperature of solvent dropped only a few degrees. To avoid heat loss, the line between the Cu coil and the glove box was shortened and the line between the outside coil and the inside coil was insulated by glass wool. As a result, the temperature of diethyl ether in the flask was lowered to -35°C, which is required for the purification of the final Mo complex.

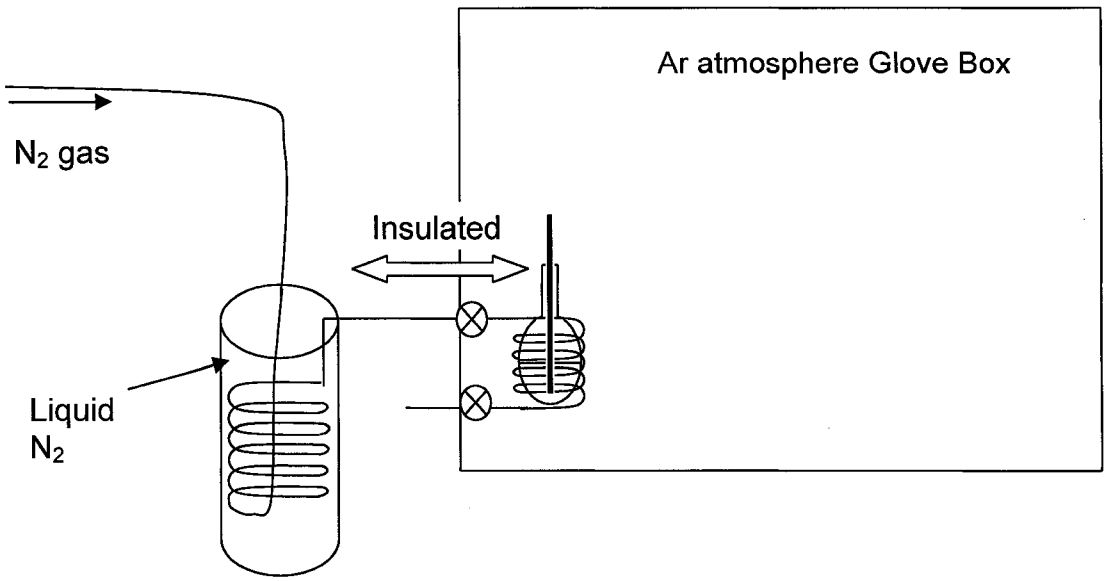

Figure 19. A cooling system in the glove box.

4.5.1 Experimental Procedure

All operations were performed in a glove box under an atmosphere of purified argon. Anhydrous Et_2O and Celite were purchased from Fisher. Pentane was purchased from Pharmco. Celite was activated in vacuo overnight at a temperature above 180°C. Pentane was shaked with conc. H_2SO_4 and preliminary dried with $CaCl_2$ followed by distiling from CaH_2 under argon. Et_2O was sparged with argon. Li(N[1-Ad]Ar)(OEt_2)(6.44 g, 19.2 mmol) and 75 ml of Et_2O were added to a 250-ml flask. The mixture was stirred for 5 min at room temperature, and then $MoCl_3(THF)_3$ (3.54 g, 8.5 mmol) was added in one portion. The reaction mixture darkened and attained a light-brown color after 5.5 h, at which time it was filtrated through Celite in order to remove LiCl and excess $MoCl_3(THF)_3$. The filtrate was stored at -35°C to precipitate out a small

quantity of solid. The mixture was then filtered through a sintered glass frit, and the filter cake was washed with pentane until the washings were colorless. The orange washings and filtrate were combined, and the cooling/filtration/extraction process was repeated for removal of the free ligand HN[1-Ad]Ar. The purification was complicated because both $Mo(N[1\text{-}Ad]Ar)_3$ and HN[1-Ad]Ar have similar solubility in pentane and in Et_2O. After solvent removal in vacuo, the residue was extracted with Et_2O (25ml). The extract was stored at 28°C until light orange solid precipitated. The solid was collected on a glass sintered frit and dried in vacuo (Figure 20). Yield 1.73 g (24%).

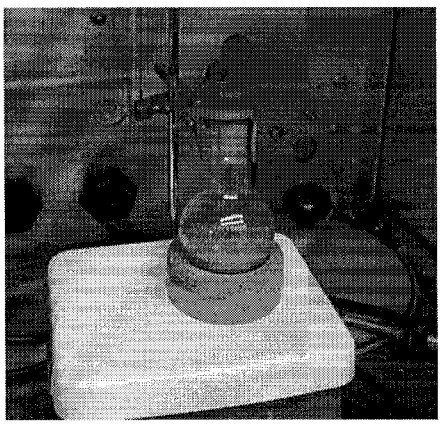

Figure 20. Synthesized $Mo(N[1\text{-}Ad]Ar)_3$

4.5.2 Physicochemical Characterization of $Mo(N[1\text{-}Ad]Ar)_3$

The obtained orange powder was measured by Micromass Time of Flight Mass Spectrometer (TOFMS) with a Solid Direct Insertion Probe. The Temperature of the probe was heated at 100°C/min to 650°C. The base peak (the largest peak) was M/Z 725.3344 and the isotopic distribution (bottom) matched with the calculated pattern (above) for $C44H57N3Mo^+$, which corresponded to an ion which lost one adamantyl

group from Mo(N[1-Ad]Ar)$_3$ (Figure 21, 22). Similarly, M/Z 859.4890 was of an ion that lost a proton from Mo(N[1-Ad]Ar)$_3$ (Figure 21, 23). Other fragmentation patterns were also consistent with the structure of Mo(N[1-Ad]Ar)$_3$. Consequently, the synthesized powder was identified as Mo(N[1-Ad]Ar)$_3$.

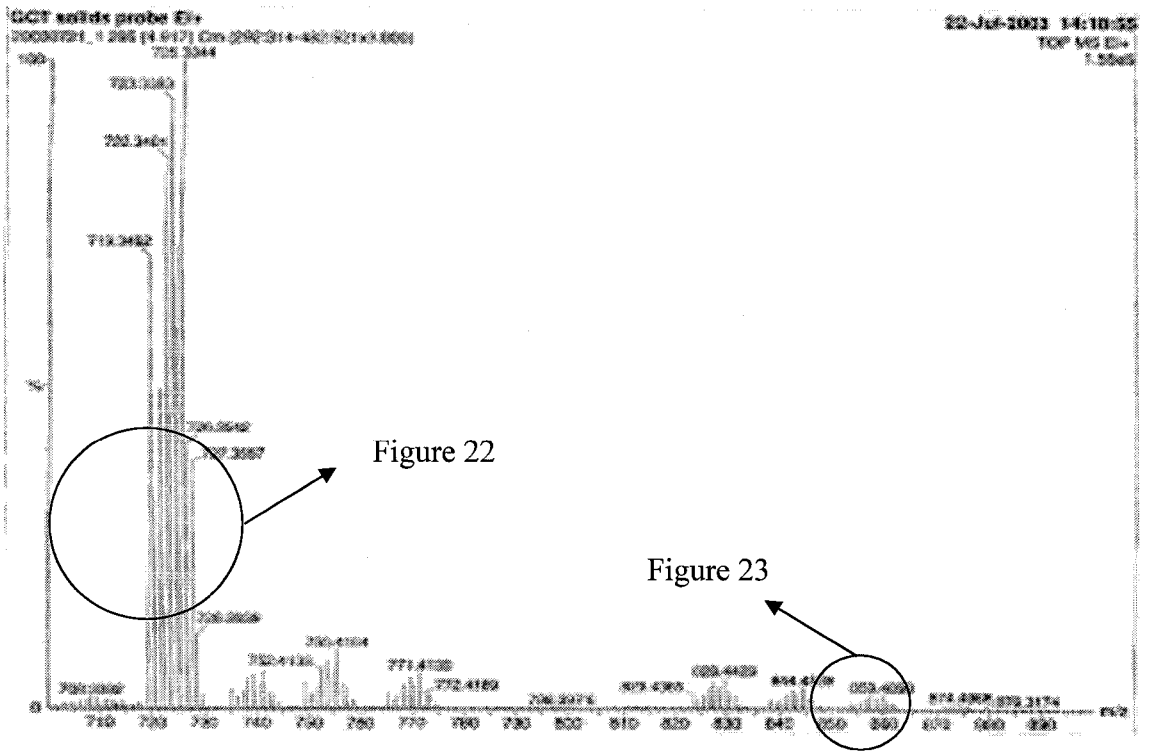

Figure 21. Identification of Mo(N[1-Ad]Ar)$_3$ by TOFMS.

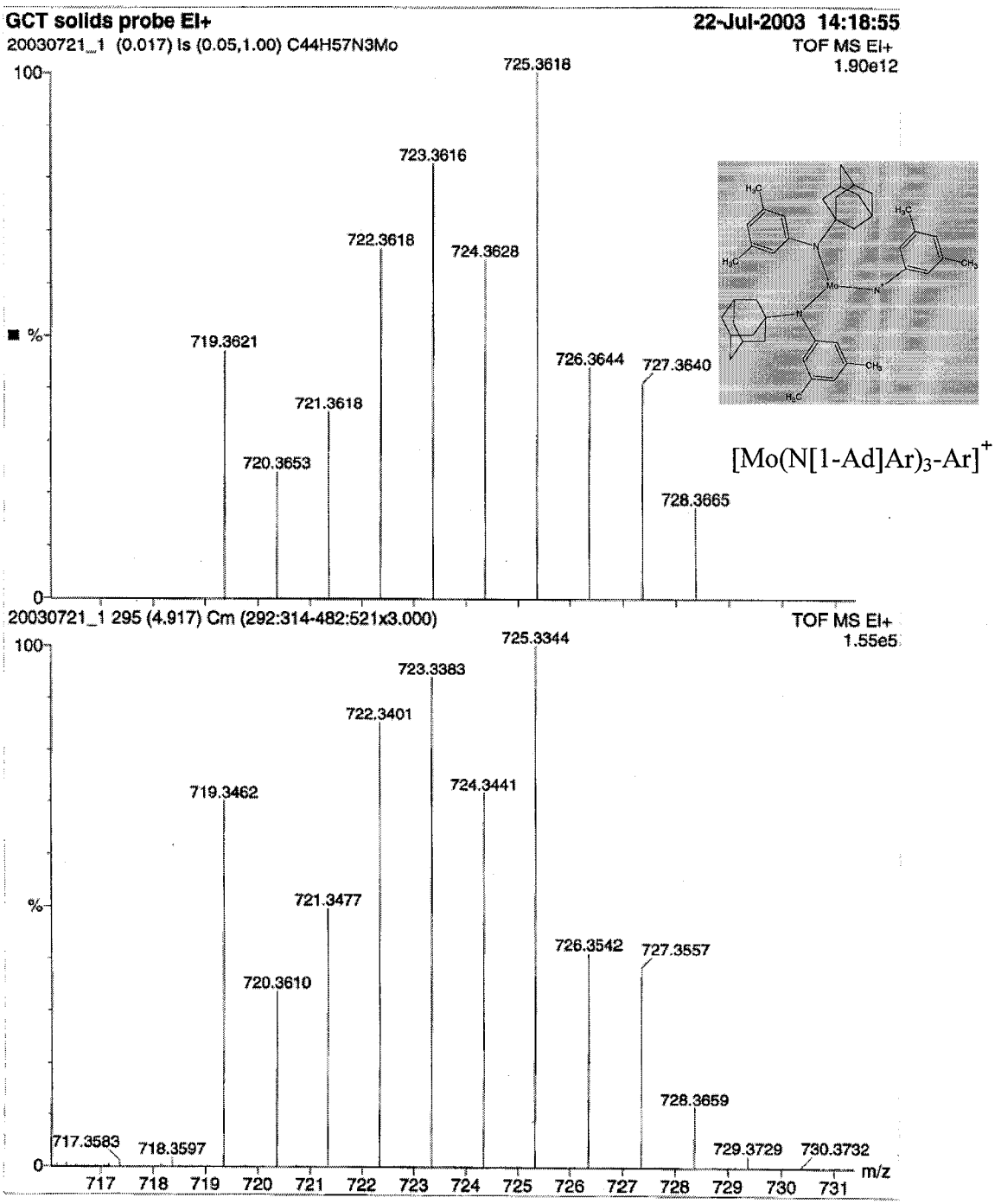

Figure 22. The measured isotopic distribution (bottom) and the calculated pattern (above) for $[Mo(N[1\text{-}Ad]Ar)_3\text{-}Ar]^+$.

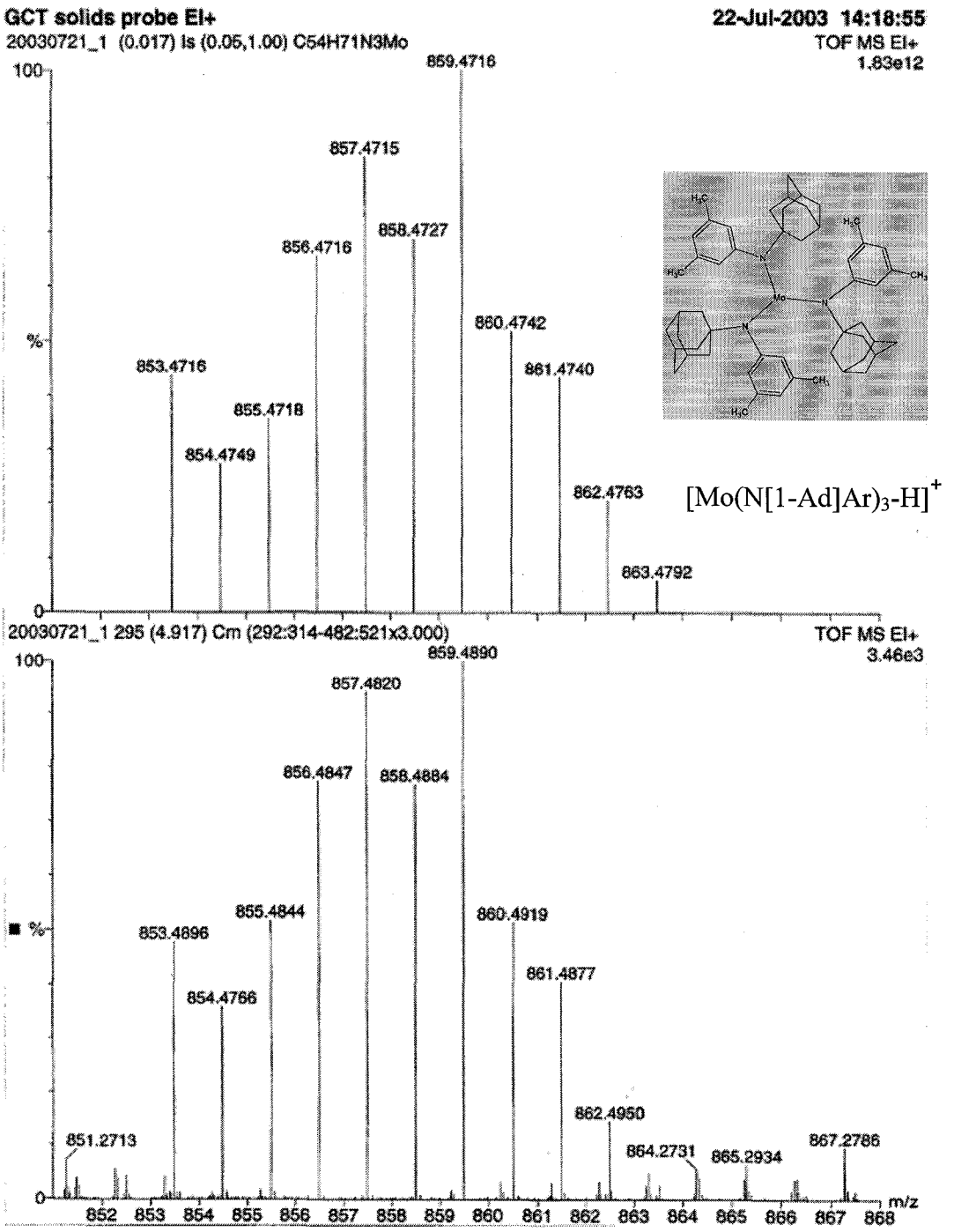

Figure 23. The measured isotopic distribution (bottom) and the calculated pattern (above) for $[Mo(N[1\text{-}Ad]Ar)_3\text{-}H]^+$.

A X-ray diffraction pattern was measured two weeks after synthesis which showed that the original complex decomposed and that this decomposition was very rapid when the compound was exposed to air.

Chapter 5

Conclusion and Discussion

The target Mo(III) complex, $Mo(N[1\text{-}Ad]Ar)_3$ was successfully synthesized. However, the complex rapidly decomposed on contact with air or moisture. Therefore, the study of adsorption and desorption of N_2, CO_2, and other gas impurities was not feasible. Improvement of stability is critical for the practical application of these unique N_2-binding complexes for N_2 separation from flue gas. Before discussion of strategies of stabilization, the reason why $Mo(N[1\text{-}Ad]Ar)_3$ was decomposed should be elucidated.

Generally, the decomposition of metal complexes is caused by oxidation of the metal center and/or formation of O_2- or N_2- bridged dimers. In the case of $Mo(N[1\text{-}Ad]Ar)_3$, the cause of decomposition is likely to be oxidation of the metal center since the undesirable dimerization is prohibited by steric hindrance of adamantyl groups attached to the ligands. Since O_2 is smaller in size than N_2, preventing only O_2 from approaching to the molybdenum center using bulkier substituents is not possible. Metal complexes known as good oxygen carriers contain ligands which are strong electron-donors (Figure 24) [57]. The electron density on the metal center appears to be the major factor in determining O_2 affinity [58]. Thus, the binding of O_2 to Mo must be sensitive to the electron-withdrawing or electron-donating ability of the ligands.

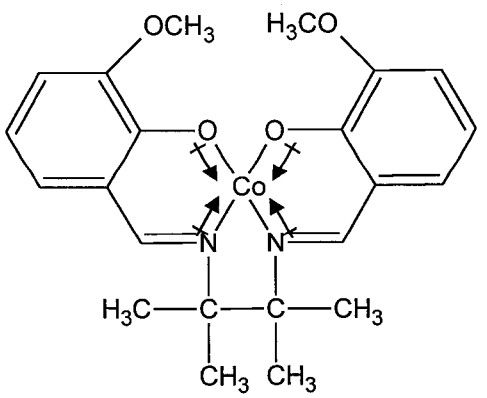

Figure 24. Oxygen-complexing carrier compound Co(3-MeOsaltmen).

The five-co-ordinate molybdenum complex, $Mo(CO)_3(PCy_3)_2$, (Cy = cyclohexyl), which can reversibly coordinate a N_2 molecule but not a O_2 molecule, was reported by Kubas [59]. This Mo(V) complex has three carbonyl ligands (CO) and two tricyclohexylphosphine (PCy_3). To know the electron density of the Mo center, the electronic properties of theses ligands and amido ligands (NR_2) are compared (Figure 25, 26).

Electronegativity is a measured of the ability of an atom to attract the shared electrons in a chemical bond. For C-O, the electronegativity difference is 2.5 – 3.5 = -1.0. Oxygen is much more electronegative than carbon, so that electrons are attracted more strongly by the oxygen atom. Because of electron withdrawal by the oxygen, carbonyl carbon is electron deficient, which produces electron-withdrawing character of the carbonyl groups. For P-C, the electronegativity difference is 2.1 - 2.5 = -0.4, that is, carbon is more electronegative than phosphorous. Although phosphorous has a lone electron pair, electron-donating property of PR_2 (R = alkyl) is not strong.

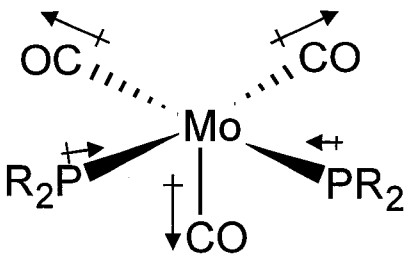

Figure 25. Electron-donating and withdrawing property of CO and PCy_3 ligands.

In contrast, for N-C, it is 3.0 – 2.5 = 0.5, i.e. nitrogen is more electronegative than carbon and nitrogen has a lone electron pair. Therefore, NR_2 is classified as a strong

electron-donating group. The electron-withdrawing groups such as CO decrease electron density on the metal (Figure 25), resulting in the lower oxygen affinity, whereas electron-donors such as NR_2 promote oxygenation by increasing the electron density (Figure 26). The synthesized Mo(III) has three amido groups which are strong electron donor ligands. Consequently, the Molybdenum center has high electron density and attracts dioxygen moleculars.

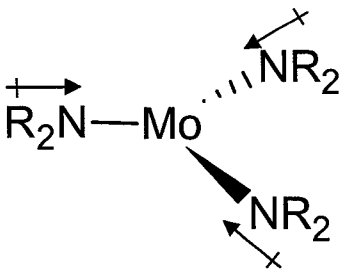

Figure 26. Electron-donating property of amido ligands.

Chapter 6

Strategies for Stabilization of N_2-binding Mo Complexes

The approaches to make the metal complexes stabilized are reviewed in this chapter. As discussed in the previous sections, there are two pathways to decompose metal complexes: one is dimer formation and another is oxidation of the metal center.

6.1 Prevention of Dimer Formation

In this work, a bulky substitute, adamantyl was used to avoid the decomposition of the Mo(III) complex. Beside introduction of bulky substitutes, immobilization of the metal complexes in various materials such as zeolite, porous organic matrix, polymer, and SiO_2 has been used for preventing aggregation of metal complexes.

6.1.1 Zeolites as Porous Hosts

The three-dimensional pore structure of zeolites provides the site for preparing a complex inside the pore. There have been several reports in the literature on Co(II) complexes in zeolite cavities. Herron has synthesized pyridine-bound Co(salene) in zeolite Y [60] (Figure 27). Metal ions and ligands may easily enter zeolite cages, but once formed inside the cages the final assembled coordination complex is too large and rigid to leave. The encapsulation is described as making a "ship-in-a-bottle" complex.

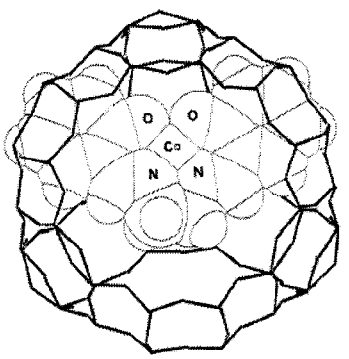

Figure 27. Pictorial representation of the Co(salene) in zeolite Y [60].

Even though Herron found out later that the Co complex was not located in the zeolite pores and withdrew his report, his approach was followed by many researchers. Various ligands such as tetraethylenepentaamine, (bis(salicylaldehyde) methylnitrilodipropyl-diimine), and (bis(acetylacetone) methyl-nitrilodipropyldiimine) have been investigated to increase the number of the active sites in this system [61, 62]. Taylor et al. has reported the synthesis of an anionic Co(II) cyanide complex in zeolites [63]. Zeolite Y with $1.5 < Si/Al < 18$ is resistant to treatments in solutions of pH 2-12 and retains its structure and crystallinity when subjected to water vapor at 410°C [64]. Each supercage of this zeolite has four 12-ring apertures, which provides N_2 permeance of 0.3 to 1.56 $\mu mol/m^2 \cdot s \cdot Pa$ [65], which is similar to the estimated value for the Mo(III) complex deposited inside modified silica membranes. The cost of zeolites is expected to be about 10% of that of the membrane and support manufacturing.

6.1.2 Organic Hosts

The template copolymerization methods are used to design and synthesize Co(II) complexes in a porous organic host [66] (Figure 29). The approach consists of 3 steps: (A) preparation of the template metal complex, (B) polymerization for immobilization of the template in porous methacrylate matrix, (C) removal non-polymerizable ligand to form void spaces for active sites (Figure 28).

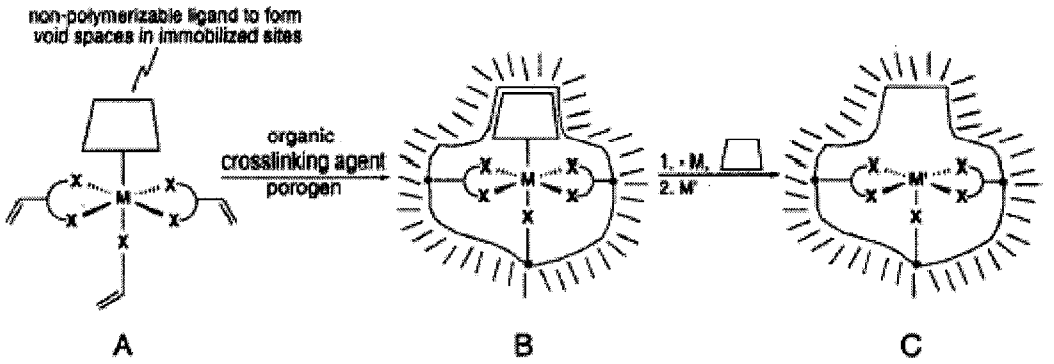

Figure 28. Preparation steps for the immobilized metal complex in porous hosts [66].

The template complex has the requisite feature for forming the immobilized metal sites: (1) three appended vinyl groups for three-point immobilization; (2) non-polymerizable ligand to form void spaces in immobilized sites; (3) substitution-inert under the conditions of polymerization.

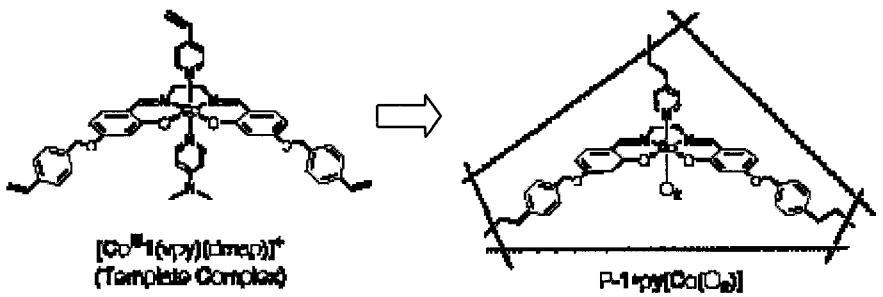

Figure 29. The Co(II) complex immobilized in organic pore [66].

Tsuchida et al. have succeeded in the facilitated oxygen transport via Co porphyrins fixed in solvent–free polymer [67]. The Co porphyrin bonded to the polymers acts as the fixed carriers of O_2 and the permeability ratio of O_2 against N_2 is > 10. This approach was followed for the nitrogen carrier, cyclopentadienyl dicarbonylmanganese (CpMn) fixed in polymer [68-70]. The polymer is synthesized from radical

copolymerization of a mixture of tricarbonyl(methylvinylcyclopentadienyl) manganese and octyl methacrylate.

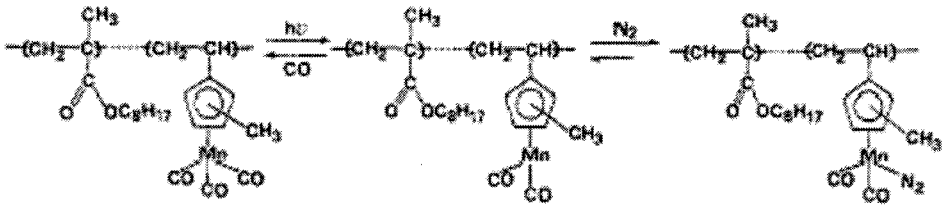

Figure 30. Cyclopentadienyl dicarbonylmanganese (CpMn) fixed in polymer [70].

By UV irradiation of the membrane in argon atmosphere, one of CO ligands is removed, which affords one vacant coordination site, and it can bind molecular N_2 rapidly and reversibly even in the solid state (Figure 30). Methacrylate polymers have great resistance to both acidic and alkaline chemicals but readily depolymerize at temperatures greater than 300°C [71]. Below glass transition temperature (T_g), polymers are stiff, hard, brittle and glass like; above the Tg, they are relatively soft, limp, stretchable, and elastic. Selection of materials with low manufacturing cost and with low T_g temperature for yielding a transparent and flexible membrane might not be difficult. However, low solubility and diffusivity of N_2 in backbone polymer materials result in a lack of physical permeation. N_2 permaence of the CpMn membrane is as low as 2.8×10^{-5} $\mu mol/m^2 \cdot s \cdot Pa$ [70].

6.1.3 Metal Complex Imprinting in SiO_2

Organic polymers tend to be fragile in organic solvents, in the presence of oxidants, or at high temperature, whereas oxide supports are inert and robust materials. A combination of two methods, namely 1) metal-complex attaching and 2) molecular

imprinting by chemical vapor deposition (CVD) at oxide surfaces was employed to prepare SiO_2-attached Rh-complex (Figure 31) [72].

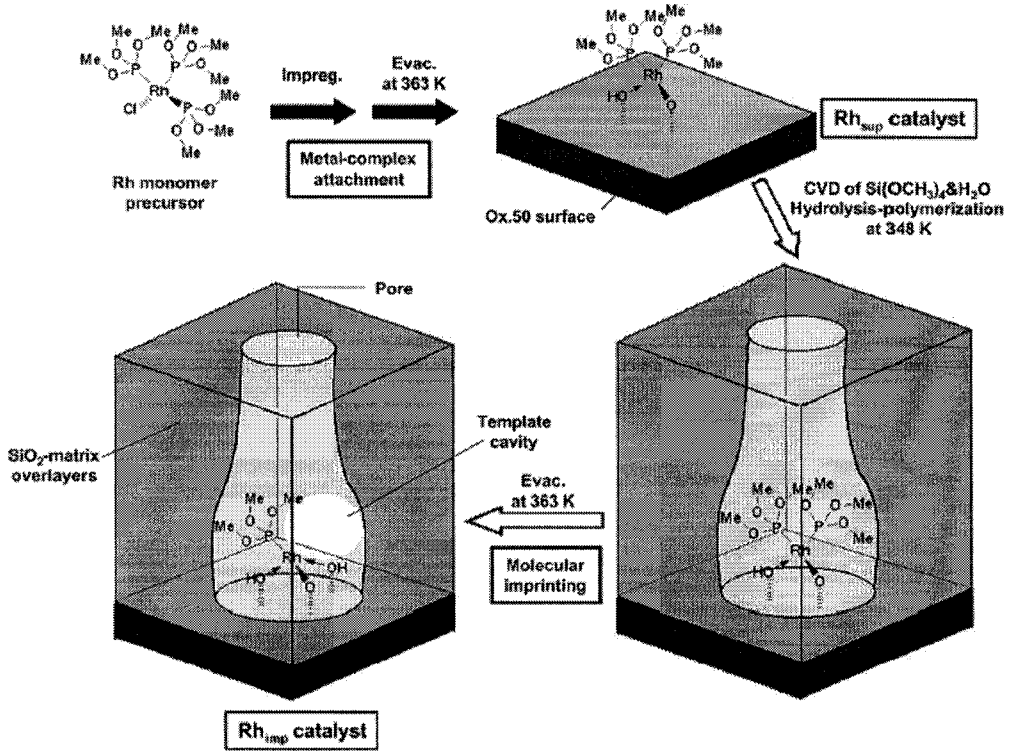

Figure 31. Preparation steps for the imprinted Ph-complex in SiO_2 [72].

Porosity of SiO_2 is preserved at relatively high temperature; however, it is readily dissolved in acidic and alkaline media. The price of $Si(OMe)_4$ is 5 times that of zeolites. This material cannot be utilized for membranes because all pores are one-dimensional and the pore openings are blocked with SiO_2.

The above approaches with the exception of the zeolite host require not only functional groups such as –OH and vinyl groups for anchoring, but also inert metal complexes under immobilization conditions such as polymerization, thermal treatment, and CVD. Preparing metal complexes with the ability to bind N_2, which also satisfied the

requirements for the immobilization, is very difficult. However, zeolites might be used as the host material to prohibit dimerization for N_2-binding metal complexes because the metal complexes are assembled inside the pores.

6.2 Prevention of Oxidation

It was shown that decreasing electron density of the metal center is effective to avoid oxidation. Beside the electron density, the number of valence electrons greatly affects the stability of metal complexes. Transition metals have 9 valence orbitals, 1s + 3p + 5d and each orbital can be filled two electrons. Metal complexes with 18 valence electrons are predicted to be particularly stable because they will have a closed shell of electron. Complexes with 18 electrons are referred as being coordinatively saturated. A molybdenum atom has 5 electrons in the 4d orbitals and one electron in the 5s orbital and the sum of the valence electrons is 6. To obey the 18 electrons rule, ligands need to donate 12 electrons in total. In the case of $Mo(N[1\text{-}Ad]Ar)_3$, each amido ligand donates 1 electron, the sum of valence electrons and ligands electrons are 9. Even after binding dinitrogen, the number of electrons is still 11 (Figure 32) and the Mo(III) complex have vacant coordination sites to react with other moleculres such as dioxygen. On the other hand, the five-co-ordinate molybdenum complex, $Mo(CO)_3(PCy_3)_2$, (Cy = cyclohexyl), which can reversibly coordinate a N_2 molecule, has 16 electrons because the CO and PCr_3 ligand donate two electrons each. After binding dinitrogen, the complex has 18 electrons and is coordinatively saturated (Figure 32). Replacement of three amido ligands with three CO and two PCy_3 ligands for the molybdenum complex is effectual on

decreasing not only the affinity of oxygen but also the reactivity of molybdenum complexes after N_2 binding.

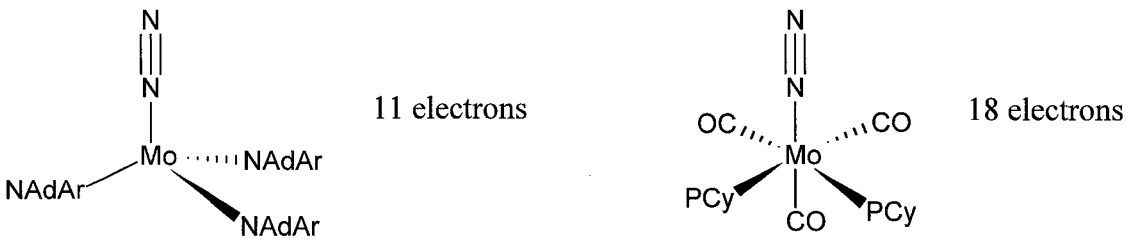

Figure 32. Electron configurations of $N_2[Mo(N[1\text{-}Ad]Ar)_3]$ and $Mo(CO)_3(PCy_3)_2$.

Chapter 7

Future Work

In order to prevent metal complexes from being oxidized, the electron density of metal center should be sufficiently low and the electron configuration should be coordinatively saturated after N_2 binding. Although the five-co-ordinate molybdenum complex $[Mo(CO)_3(PR_3)_2]$ satisfies these requirements, this complex might be not stable due to dimerization. We propose two approaches to avoid dimerization of the N_2-binding complex $Mo(CO)_3(PCy_3)_2$.

Approach 1: Utilization of Bulky Substituent

As seen in Figure 33, the structure of N_2-briged dimer μ-$N_2[Mo(CO)_3(PCy_3)_2]_2$ is already very crowded. If the ligands have slightly bulkier substituents, the formation of dinuclear compounds would be averted by their steric hindrance. By employing phosphine ligands with dimethylcyclohexyl or adamantyl groups instead of cyclohexyl substituted phosphine, it will be achivable.

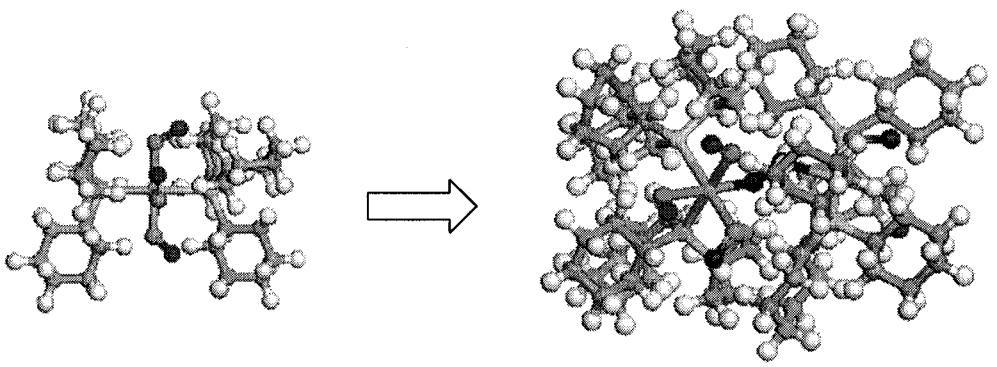

$Mo(CO)_3(PCy_3)_2$ μ-$N_2[Mo(CO)_3(PCy_3)_2]_2$

Dimethylcyclohexyl Adamantyl

Figure 33. Stabilization of the N_2 binding Mo complex by bulker substituents.

Approach 2: Utilization of Zeolite as a Host Material

The three-dimensional pore structure of zeolite is particularly attractive because the site isolation prevents aggregation of metal complexes. Generally, zeolites are classified into small, medium, and large pore materials according to the size of the pore openings [73]. The pore is designated an n-ring, where n is the number of T-atoms and T is an aluminum or silicon atom. Small pore structures are 8-membered rings, medium pore zeolites have 10-membered rings, large pore frameworks are 12-membered rings. Some zeolites have pores with 14-, 18- , and 20-membered rings, but they are very rare. Typical zeolites are shown in Figure 34.

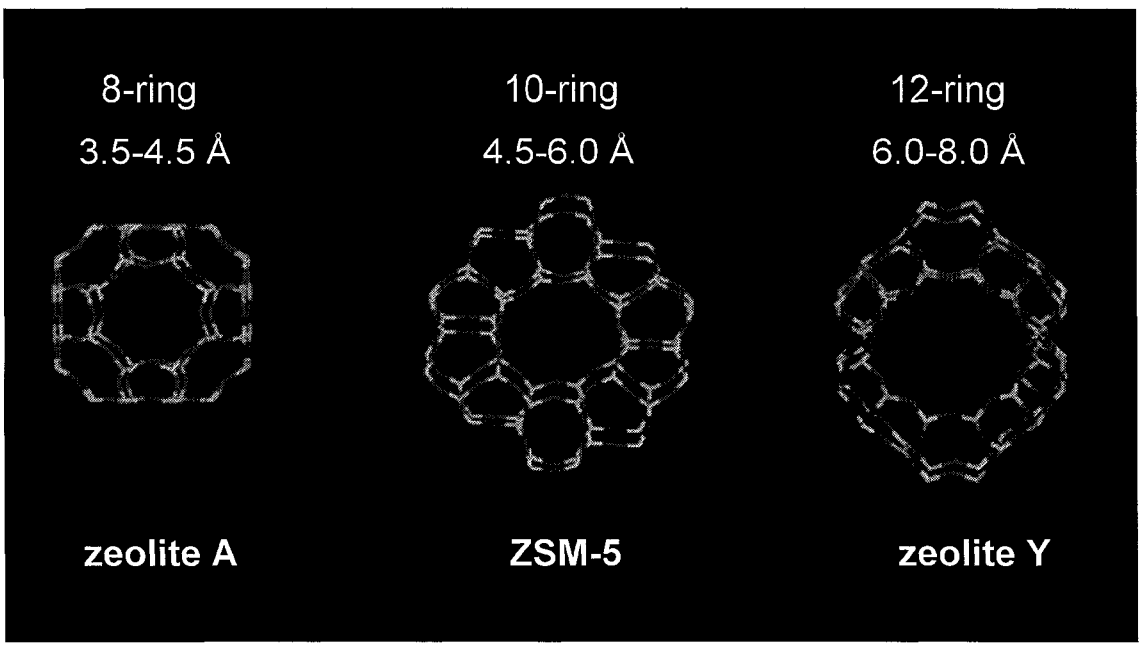

Figure 34. Pore opening structures of typical zeolites.

Zeolite A

Zeolite A exhibits the LTA (Linde Type A) structure. It has a 3-dimensional pore structure with pores running perpendicular to each other in the x, y, and z planes. The pore diameter is defined by an eight member oxygen ring and is small at 4.2Å. This leads into a supercage of minimum free diameter 11.4Å.

ZSM-5

ZSM-5 has two types of pores, both formed by 10-membered oxygen rings. The first of these pores is straight and elliptical in cross section, the second pores intersect the straight pores at right angles in a zigzag pattern. Linear channels have a diameter of 5.1 x 5.6 Å which are perpendicular arranged to zigzag channels with a diameter of 5.4 x 5.6 Å.

Zeolite Y

Zeolite Y has a 3-dimensional pore structure with pores running perpendicular to each other in the x, y, and z planes similar to LTA. The pore structure is characterized by supercages approximately 12Å in diameter, which are linked through windows about 7.4 Å in diameter composed of rings of a 12-membered oxygen ring. These cages and pores permit access to quite large molecules.

For synthesis of "ship in bottle" complexes, zeolite should have a cage to trap the complex and the pore opening should be adequately large for the ligands to enter but not for the complex to pass through. In the case of ZSM-5, their voids are channels rather than cages. Although zeolite A has supercages, 8-membered pore openings are too small for ligands to enter the cage because ligands are usually bigger than 5 Å. Zeolite Y has pore openings about 7.4 Å which lead into a supercage of diameter 12Å. This structure of zeolite Y is suitable for in site complexation. Therefore, we considered encapsulation

of the N_2-binding complex $Mo(CO)_3(PCy_3)_2$ in zeolite Y (Figure 35). In most cases, the zeolite is first exchanged with the transition metal ion and then the zeolite is exposed to the ligand. With using the ion exchange method, however, the amount of Mo ions added to the zeolite is as low as 8.5% of the exchange capacity [74]. Thus, we use the method, which can introduce molybdenum into zeolites by adsorption of molybdenum hexacarbonyl. Substitution reactions of $Mo(CO)_6$ with PMe_3 in the cages of a zeolite Y host proceed cleanly to form $Mo(CO)_4(PMe_3)_2$, (Me = methyl) [75]. Similarly, when commercially available P^tBu_3 (^{t}Bu = tert-butyl) instead of PMe_3 is utilized, $Mo(CO)_4(P^tBu_3)_2$ might form in the cage. Indeed, the complex, $Mo(CO)_4(PR_3)_2$ has been synthesized by the reaction of $Mo(CO)_6$ with PR_3 in solution [76]. The size of $Mo(CO)_4(P^tBu_3)_2$ is estimated to be 11.3 Å so that the use of zeolite Y with 12 Å large supercages is suitable [73]. The once flexible ligands, with a diameter of < 7 Å have been locked into a complex, the formed complex $Mo(CO)_4(P^tBu_3)_2$ is too large to leave the supercage by diffusion. After one of CO ligands removed by UV irradiation, $Mo(CO)_3(P^tBu_3)_2$, which is analogous to $Mo(CO)_3(PCy)_2$ known as a N_2 binding complex [59], is expected to be produced inside zeolite. Disadvantage of this material is that it is necessary to remove moisture from flue gas before the separation since zeolites are extremely sensitive to the presence of moisture.

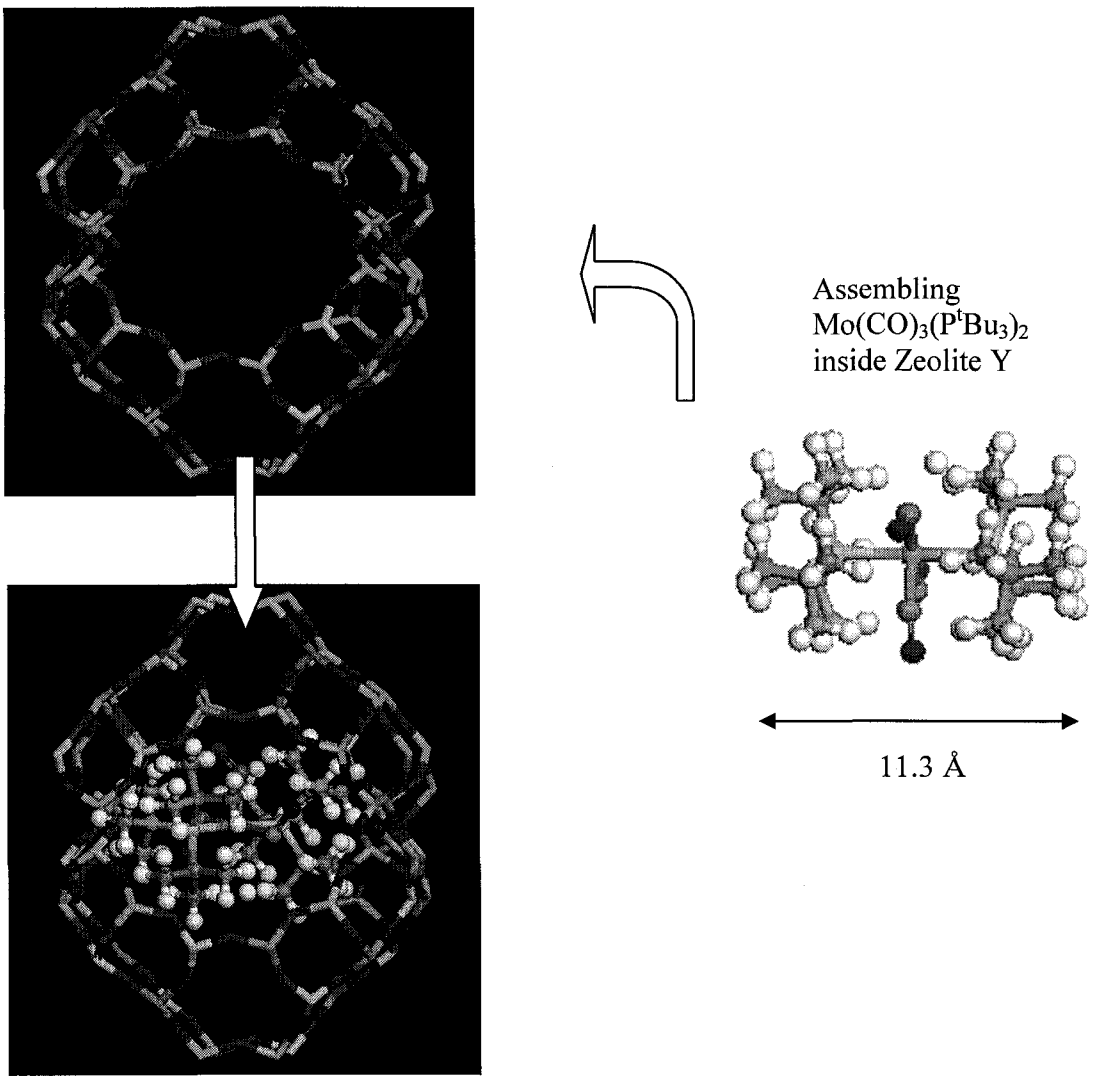

Figure 35. Stabilization of the N_2 binding Mo complex by zeolite Y.

Bibliography

1. Report, "*Research and development needs for the sequestration of carbon dioxide as part of a carbon management strategy*", The National Coal Council, US DOE, Washington, DC, May 2000.

2. H. J. Herzog, *Environmental Science and Technology*, 2001, **35**, 148A.

3. R. W. Baker, *Ind. Chem. Eng. Res.*, 2002, **41**, 1393.

4. S.I. Plasynski and Z.-Y. Chen, Abstracts of Papers of the American Chemical Society, 2000, **220**, U391.

5. R. N. Maddox, G. J. Mains and M. A. Rahman, *Ind. Eng. Chem. Res.*, 1987, **26**, 27.

6. T. Mimura, S. Shimojo, T. Suda, M. Iijima and S. Mitsuoka, *Energy Convers. Mgmt.*, 1995, **36,** 397.

7. T. Mimura, H. Simayoshi, T. Suda, M. Iijima and S. Mituoka, *Energy Convers. Mgmt.*, 1997, **38,** S 57.

8. S. Satyapal, T. Filburn, J. Trela and J. Strange, *Energy & Fuels*, 2001, **15,** 250.

9. H. Y. Huang and R. T. Yang, *Ind. Eng. Chem. Res.*, 2003, **42,** 2427.

10. O. Leal, C. Bolivar, C. Ovalles, J. J. Garcia, Y. Espidel, *Inorganica Chimica Acta*, 1995, **240**, 183.

11. R. Barker, *J. Appl. Chem. Biotechnol.*, 1973, **23**, 733.

12. H. Gupta and L. -S. Fan, *Ind. Eng. Chem. Res.*, 2002, **41**, 4035.

13. W. J. Koros and G. K. Fleming, *J. Membr. Sci.*, 1993, **83**, 1.

14. R. E. Kesting and A. K. Fritzsche, Polimeric Gas Separation Membranes, John Wiley & Sons, Inc., 1993.

15. H. Chen, A. S. Kovvali, S. Majumdar and K. K. Sirkar, *Ind. Eng. Chem. Res.*, 1999, **38**, 3489.

16. P. H. M. Feron and A. E. Jansen, *Energy Convers. Mgmt.,* 1997, **38**, S 93.

17. M. P. Bernal, M. Bardají, J. Coronas and J. Santamaría, *J. Membr. Sci.,* 2002, **203**, 209.

18. M. J. Cogbill and G. P. Marsh, *Energy Conversion and Management*, 1992, **33**, 487.

19. B. Coughlan, S. Kilmartin, *J. Chem. Soc., Faraday Trans. I*, 1979, **75**, 1969.

20. B. Coughlan and W. McCann, *J. Chem. Soc., Faraday Trans. I*, 1975, **71**, 1809.

21. D. W. Breck, *Zeolite Molecular Sieves, Krieger*, Malabar, FL, 1984.

22. J. Pires, M. B. Decarvalho, F. R. Ribeiro, E. G. Derouane, *J. Molec. Catal.,* 1993, **85**, 295.

23. S. Kim, C. Gauer, V.V. Guliants and Y.S. Lin, "Amine-modified mesoporous silica membranes for separation of carbon dioxide under ambient conditions", Annual 2002 AIChE Meeting, Indianapolis, Nov. 3-8, 2002.

24. V.V. Guliants, S. Kim, C. Gauer, and Y.S. Lin, "Amine-modified mesoporous silica membranes for separation of carbon dioxide under ambient conditions", 7th International Conference on Inorganic Membranes, Dalian, China, June 23-26, 2002.

25. C. E. Laplaza and C. C. Cummins, *Science*, 1995, **268**, 861.

26. C. E. Laplaza, A. L. Odom, W. M. Davis and C. C. Cummins, *J. Am. Chem. Soc.,* 1995, **117**, 4999.

27. C. E. Laplaza, M. J. A. Johnson, J. C. Peters, A. L. Odom, E. Kim, C. C. Cummins, G. N. George and I. J. Pickering, *J. Am. Chem. Soc.,* 1996, **118**, 8623.

28. C. C. Cummins, *Chem. Commun.,* 1998, 1777.

29. G. Ertl, in *Catalytic Ammonia Synthesis*, Jennings, J. R. Eds., Plenum, New York, 1991, p109.

30. J. Chatt, J. R. Dilworth and R. L. Richards, *Chem. Rev.,* 1978, **78**, 589.

31. K. Marchal and J. Vanderleyden, *Biol Fertil Soil,* 2000, **30**, 363.

32. D. V. Yandulov and R. R. *Schrock, Science,* 2003, **301**, 76.

33. A. D. Allen and C . V. Senoff, *Chem. Commun.*, 621 (1965).

34. H. Seino, Y. Ishii, T. Sasagawa, M. Hidai, *J. Am. Chem. Soc.,* 1995, **117**, 12181.

35. H. Masanobu and M. Yasushi, *Pure Appl. Chem.,* 2001, **73**, 261.

36. D. Sellman and G. Mailsel, *Z. Naturforsch.,* 1972, 465.

37. D. Sellman, Angew. *Chem., Int. Ed. Engl.,* 1971, **10**, 919.

38. D. Sellman, *J. Organomet. Chem.,* 1972, **36**, C27.

39. Yu G. Borodko, I. N. Ivleva. L. M. Kachapina, S. J. Salienko, A. K. Shilova, and A. E. Shilov, *J. Chem. Soc., Chem. Commun.,* 1972, 1178.

40. J. Manriquez and J. E. Bercaw, *J. Am. Chem. Soc.,* 1974, **96**, 6229.

41. M. B. O'Donoghue, N. C. Zanetti, W. M. Davis, and R. R. Schrock, *J. Am. Chem. Soc.,* 1997, **119**, 2753.

42. M. B. O'Donoghue, W. M. Davis, and R. R. Schrock, *Inorg. Chem.,* 1998, **37**, 5149.

43. J. C. Peters, J. –P. F. Cherry, J. C. Thomas, L. Baraldo, D. J. Mindiola, W. M. Davis and C. C. Cummins, *J. Am. Chem. Soc.,* 1999, **121**, 10053.

44. J. -P. F. Cherry, A. R. Johnson, L. M. Balaldo, Y. -C. Tsai, C. C. Cummins, S. V Kryatov, E. V. Rybak-Akimova, K. B. Capps, C. D. Hoff, C. M. Haar, and S. P. Nolan, *J. Am. Chem. Soc.,* 2001, **123,** 7271.

45. Y.-C, Tsai, M. J. A.Johnson, D. J. Mindiola, C. C.Cummins, W. T. Klooster, and T. F. Koetzle, *J. Am. Chem. Soc.,* 1999, **121,** 10426.

46. Q. Cui, D. G. Musaev, M. Svensson, S. Sieber and K. Morokuma, *J. Am. Chem. Soc.,* 1995, **117**, 12366.

47. A. K. Rappé, *Inorganic Chemistry,* 1984, **23**, 995.

48. D. G. Musaev, H. Basch and K. Morokuma, in Computational Modeling of Homogeneous Catalysis, Kluwer Academic publishers, 2002, p325.

49. K. M. Neyman, V. A. Nasluzov, J. Hahn, C. R. Landis and N. Rösch, *Organometallics,* 1997, **16**, 995.

50. A. R. Johnson, W. M. Davis, C. C. Cummins, S. Serron, S. P. Nolan, D. G. Musaev, and K. Morokuma, *J. Am. Chem. Soc.,* 1998, **120**, 2071.

51. A. R.Johnson and C. C. Cummins, *Inorg. Synth.,* 1998, **32**, 123.

52. K. B. P. Ruppa, N. Desmangles, S. Gambarotta, G. Yap and A. L. Rheingold, *Inorg. Chem.,* 1997, **36**, 1194.

53. P. E. Aldrich, E. C. Hermann, W. E. Meier, M. Paulshock, W. W. Prichard, J. A. Snyder and J. C. Watts, *J. Med. Chem.,* 1971, **14**, 535.

54. J. R. Dilworth and R. L. Richards, *Inorg. Synh.,*. 1980, **20,** 119.

55. F. Stoffelbach, D. Saurenz, and R. Poli, *Eur. J. Inorg. Chem.,* 2001, 2699.

56. R. Poli and H. D. Mui, *J. Am. Chem. Soc.,* 1990, **112**, 2446.

57. B. M. Johnson, R. W. Baker, S. L. Matson, K. L. Smith, I. C. Roman, M. E. Tuttle, and H. K. Lonsdale, *J. Membr. Sci.* 1987, **31**, 31.

58. I. K. Meier, R. M. Pearlstein, D. Ramprasad, and G. P. Pez, *Inorg. Chem.* 1997**, 36**, 1707.

59. G. J. Kubans, *J. Chem. Soc., Chem. Comm.,* 1980, 61.

60. N. Herron, *Inorg. Chem.,* 1986, **25**, 4714.

61. P. K. Dutta and C. Bowers, *Langumuir,* 1991, **7**, 937.

62. D. E. De Vos, E. J. P. Feijen, R. A. Schoonheydt, and P. A. Jacobs, *J. Am. Chem. Soc.,* 1994, **116**, 4746.

63. R. J. Taylor, R. S. Drago, and J. P. Hage, *Inorg. Chem.,* 1992, **31**, 253.

64. M. Briend-Faure, O. Cornu, D. Delafosse, R. Monque, and M. J. Peltre, *Applied Catalysis,* 1988, **38**, 71.

65. A. Tavolaro and E. Drioli, *Adv. Mater.* 1999, **11**, 975.

66. A. C. Sharma and A. S. Borovik, *J. Am. Chem. Soc.,* 2000, **122**, 8946.

67. H. Nishide, M. Ohyanagi, O. Okada, and E. Tsuchida, *Macromolecules,* 1987, **20**, 417.

68. C. U. Pittman Jr., G. V. Marlin, T. D. Rounsefell, *Macromolecules,* 1973, **6**, 1.

69. Y. Kurimura, F. Ohta, J. Gohda, H, Nishida, and E. Tsuchida, *Makromol. Chem.,* 1982, **183**, 2889.

70. H. Nishide, H. Kawakami, Y. Kurimura, and E. Tsuchida, *J. Am. Chem. Soc.,* 1989, **111**, 7175.

71. H. F. Mark, *Encyclopedia of Polymer Science and Engineering*,Wiley, v1, 1985.

72. H. O. Pastore, G. A. Ozin, and A. J. Poë, *J. Am. Chem. Soc.,* 1993, **115**, 1215.

73. H. van Bekkum, *Introduction to Zeolite Science and Practice*, Elsevier, 2001.

74. P. E. Dai and J. H. Lunsford, *J. Catal.,* 1980, **64**, 173.

75. M. Tada, T. Sasaki, and Y. Iwasawa *Phys. Chem. Chem. Phys.,* 2002, **4**, 4561.

76. E. C. Alyea, G. Ferguson, and S. Kannan, *Acta Cryst.,* 1996, **C52**, 765.